

Dianilinophthalimides: Potent and Selective, ATP-Competitive Inhibitors of the EGF-Receptor Protein Tyrosine Kinase

Uwe Trinks, Elisabeth Buchdunger, Pascal Furet, Wilhelm Kump, Helmut Mett, Thomas Meyer, Marcel Müller, Urs Regenass, Greti Rihs, Nicholas Lydon, and Peter Traxler*

CIBA Pharmaceuticals Division, Oncology and Virology Research Department, Ciba-Geigy Limited, CH-4002 Basel, Switzerland

Received September 24, 1993*

Dianilinophthalimides represent a novel class of inhibitors of the EGF-receptor protein tyrosine kinase with a high degree of selectivity versus other tyrosine and serine/threonine kinases. Steady-state kinetic analysis of compound **3**, which showed potent inhibitory activity, revealed competitive type kinetics relative to ATP. Despite a highly symmetrical structure of compound **3**, X-ray studies revealed an unsymmetrical propeller-shaped conformation of the molecule which differs clearly from that of the constitutionally related staurosporine aglycons. These conformational differences may explain the reversal of the selectivity profile of compound **3** relative to the staurosporine aglycons. In cellular assays compounds **3** and **4** have been shown to inhibit EGF-induced receptor autophosphorylation, *c-fos* induction and EGF-dependent proliferation of Balb/c MK cells. This inhibition was selective as compounds had no effect on PDGF-induced receptor autophosphorylation and *c-fos* induction. Furthermore, compound **3** showed potent antitumor activity *in vivo* at well-tolerated doses.

Introduction

The epidermal growth factor receptor (EGF-R) is a transmembrane glycoprotein that mediates the mitogenic response of cells to epidermal growth factor (EGF) and transforming growth factor α (TGF- α).^{1,2} The receptor consists of an extracellular hormone binding domain, a short hydrophobic transmembrane domain, and an intracellular region which contains a ligand-activatable protein tyrosine kinase domain.¹⁻³ Tyrosine protein kinase activity is essential for signal transduction via the EGF-R.^{4,5} The EGF-R is involved in epithelial proliferation and has been strongly implicated in malignant tumor growth.^{3,6,7} The *c-erbB1* gene, which encodes the EGF-R, has been found to undergo gene amplification or overexpression in many human tumors of epithelial or neuroepithelial origin.⁶ In addition, the closely related *c-erbB2* gene has been found to be amplified or overexpressed at high frequency in human mammary and ovarian carcinomas.⁸

The concept that deregulated signal transduction, resulting from receptor overexpression, can drive cellular transformation, is supported by many experimental findings. High-level expression of either the EGF-R^{9,10} or p185^{*c-erbB2*} in NIH 3T3 cells results in cellular transformation and tumorigenicity *in vivo*.⁹ Furthermore, transgenic animals which overexpress TGF- α further highlight the tumorigenic potential of inappropriate signal transduction via the EGF-R *in vivo*.¹²⁻¹⁴ Such experimental findings have established a mechanistic basis for the hypothesis that EGF-R or p185^{*c-erbB2*} amplification/overexpression or inappropriate mitogenic growth factor production can drive tumor growth.

The role of the EGF-R and p185^{*c-erbB2*} protein tyrosine kinases in epithelial proliferation suggests that selective enzyme inhibitors could have therapeutic potential in the

treatment of malignant and nonmalignant epithelial diseases. Due to the involvement of tyrosine kinases in many signal transduction pathways, it will be important to develop agents with high selectivity at the enzyme level.

A number of different classes of compounds have been reported as tyrosine kinase inhibitors (reviewed in ref 15). However, most compounds show limited selectivity and potency at the cellular level and low efficacy in animal models.

In the present paper, we describe the synthesis, structure-activity relationships, and biological profile of a novel group of tyrosine kinase inhibitors which preferentially inhibit signal output from the ligand-activated EGF-R and which exhibit potent antitumor activity *in vivo*.

Inhibitor Design

The microbial alkaloid staurosporine is a potent but nonselective inhibitor of many protein kinases.¹⁶⁻¹⁸ It acts as a competitive inhibitor with respect to the cofactor ATP and is noncompetitive with respect to an artificial substrate.¹⁹ On the basis of the structure of staurosporine, various aglycon and diindolylmaleimide derivatives have been synthesized.²⁰⁻²² Despite the fact that these compounds also act as competitive inhibitors relative to ATP, they exert a high degree of selectivity toward inhibition of serine/threonine kinases relative to tyrosine kinases.^{21,22} These results indicate that it is possible to design potent and selective ATP-competitive protein kinase inhibitors. In view of these facts, we have attempted the synthesis of 4,5-dianilinophthalimides as protein kinase inhibitors. In contrast to the staurosporine aglycons and the diindolylmaleimides, the 4,5-dianilinophthalimides proved to be potent and selective EGF-R protein tyrosine kinase inhibitors (Table 2). Constitutionally, staurosporine aglycons, diindolylmaleimides, and 4,5-dianilinophthalimides appear very similar (Figure 1): 4,5-dianilinophthalimides differ from staurosporine aglycons by two missing carbon-carbon bonds and from diindolylmaleimides by one missing carbon-carbon bond. However, with respect

* To whom correspondence should be addressed: Dr. Peter Traxler, Ciba Pharmaceuticals Division, Oncology and Virology Research Department, K136.4.8220, Ciba-Geigy Limited, CH-4002 Basel, Switzerland (Phone: 061/695286. Fax: 061/6967826).

* Abstract published in *Advance ACS Abstracts*, February 15, 1994.

Table 1. Data for Compounds 1-21

compd	R ₁	R ₂	R ₃	R ₄	R ₅	formula	FABMS	anal.
1	H	H	H	H		C ₂₂ H ₂₀ N ₂ O ₄	277 (M ⁺ + H)	C,H,N
2	F	F	H	H		C ₂₂ H ₂₀ F ₂ N ₂ O ₄	413 (M ⁺ + H)	C,H,N,F
3	H	H	H	H	H	C ₂₀ H ₁₆ N ₃ O ₂	330 (M ⁺ + H)	C,H,N
4	F	F	H	H	H	C ₂₀ H ₁₆ F ₂ N ₃ O ₂	366 (M ⁺ + H)	C,H,N,F
5	CH ₃	CH ₃	H	H	H	C ₂₂ H ₁₈ N ₃ O ₂	357 (M ⁺)	C,H,N
6	OCH ₃	OCH ₃	H	H	H	C ₂₂ H ₁₈ N ₃ O ₄	390 (M ⁺ + H)	C,H,N
7	OH	OH	H	H	H	C ₂₀ H ₁₆ N ₃ O ₄	362 (M ⁺ + H)	C,H,N
8	N(C ₂ H ₅) ₂	N(C ₂ H ₅) ₂	H	H	H	C ₂₈ H ₃₂ N ₅ O ₂	472 (M ⁺ + H)	C,H,N
9	I	I	H	H	H	C ₂₀ H ₁₆ N ₃ O ₂ I ₂	582 (M ⁺ + H)	HRMS
10	CN	CN	H	H	H	C ₂₂ H ₁₈ N ₅ O ₂	380 (M ⁺ + H)	HRMS
11	C ₆ H ₅	C ₆ H ₅	H	H	H	C ₃₂ H ₂₈ N ₃ O ₂	482 (M ⁺ + H)	C,H,N
12	OCH ₃	H	H	H	H	C ₂₁ H ₁₇ N ₃ O ₃	360 (M ⁺ + H)	C,H,N
13	H	H	-CH ₂ CH ₂ -	H	H	C ₂₂ H ₁₇ N ₃ O ₂	356 (M ⁺ + H)	HRMS
14	H	H	CH ₃	H	H	C ₂₁ H ₁₇ N ₃ O ₂	344 (M ⁺ + H)	HRMS
15	GH	H	CH ₃	CH ₃	H	C ₂₂ H ₁₆ N ₃ O ₂	358 (M ⁺ + H)	a
16	H	H	COCH ₃	H	H	C ₂₂ H ₁₇ N ₃ O ₃	372 (M ⁺ + H)	HRMS
17	H	H	H	H	C ₆ H ₅	C ₂₈ H ₁₈ N ₃ O ₂	405 (M ⁺)	C,H,N
18	H	H	H	H	CH ₃	C ₂₁ H ₁₇ N ₃ O ₂	344 (M ⁺ + H)	C,H,N
19						C ₂₀ H ₂₇ N ₃ O ₂	342 (M ⁺ + H)	C,H,N
21						C ₂₀ H ₁₄ NO ₂ S ₂	364 (M ⁺ + H)	HRMS

^a No elemental analysis or HRMS (only small amount of compound available).

to their physicochemical properties, conformation, and synthesis, they represent a different compound class.

Chemistry

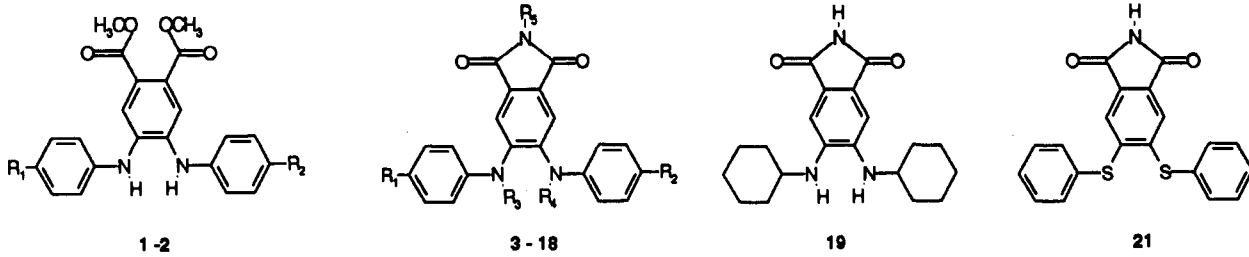
Dianilinophthalimides 3-16 [dianilinophthalimide (3) is also referred to as DAPH 1 (submitted for publication, ref 47)] were synthesized by a four-step procedure, starting from commercially available 2,3-butanedione. Silylation of 2,3-butanedione using chlorotrimethylsilane and triethylamine gave 2,3-bis((trimethylsilyl)oxy)-1,3-butadiene which by Diels-Alder reaction with dimethyl acetylenedicarboxylate led to dimethyl 4,5-bis((trimethylsilyl)oxy)cyclohexa-1,4-dienedicarboxylate. This bis-silyl enol ether reacted with different anilines to form dimethyl 4,5-dianilinophthalates 1, 2, 2a-g, which were converted directly to the corresponding phthalimides using ammonia gas and ethylene glycol as solvent (Scheme 1). Alternative methods such as copper-assisted substitution of 4,5-dichlorophthalates with anilines or anilides and reaction of anilines with 4,5-bis((trimethylsilyl)oxy)-1,2,3,6-tetrahydrophthalimide (easily accessible through a Diels-Alder reaction of 2,3-bis((trimethylsilyl)oxy)-1,3-butadiene with maleimide) failed. The former gave yields below 1% even under harsh conditions; the later resulted in the formation of tetrahydrocarbazoles.²³

Dimethyl 4,5-dianilinophthalates (1, 2, 2a-g) were synthesized from dimethyl 4,5-bis((trimethylsilyl)oxy)cyclohexa-1,4-dienedicarboxylates by a modification of the procedure described by Matlin et al.²³ with a 30-70% yield. The reaction of the bis-silyl enol ether with anilines followed a complex scheme and involved a series of tautomerizations, imine formations, and finally an oxidation step. The yield and the product profile of the reaction are heavily dependent upon the acid/aniline ratio, the temperature, and the substituents at the aniline ring.

In general, electron withdrawing groups in the 2- or 4-position of the aniline ring resulted in a large decrease in the yield. Hexamethyldisiloxane is formed during the reaction. As byproducts, dimethyl 4-anilino-5-hydroxyphthalates 22 and dimethyl 5-anilino-7-oxabicyclo[2.2.1]hept-2-ene-1,2-dicarboxylates 23 were formed (unpublished results). Small amounts of 4,5-dianilinophthalanilides (e.g. 17) were also formed (Scheme 2). The dimethyl 1,2,3,4-tetrahydrocarbazoledicarboxylates, found as main byproducts by Matlin et al.,²³ were not formed under our reaction conditions.

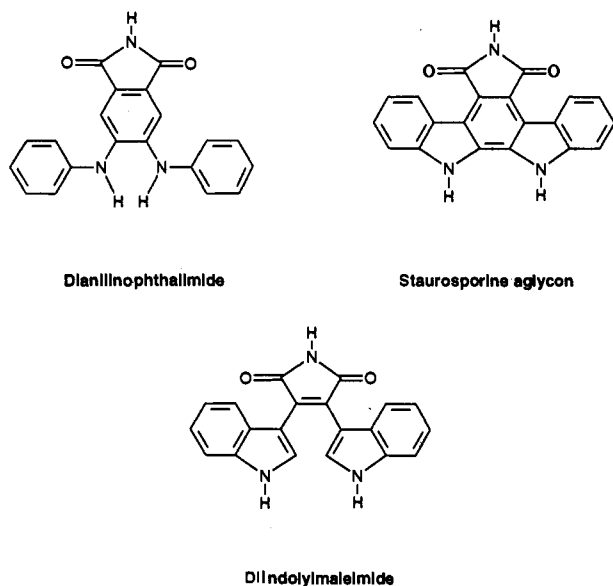
The dianilinophthalimides (3-6, 8, 9, 11-16) were synthesized from the corresponding dimethyl phthalates (1, 2, 2a-k) by treatment with an excess of ammonia gas in ethylene glycol at 120 °C (Scheme 1). The temperature and solvent were absolutely critical for this reaction: no product was isolated below a reaction temperature of 120 °C. With other alcohols as solvents (methanol, ethanol, monoglyme), trans-esterification was the main reaction. Diglycol phthalates (e.g. 24) were the main byproducts of the conversion of dimethyl phthalates to phthalimides. Due to their polar chromatography behavior, they could easily be separated from the phthalimides by flash chromatography or even simple filtration through silica gel. Other phthalates and *N*-methylphthalimides (e.g. 18) were also formed in trace amounts (Scheme 2).

The dihydroxy derivative 7 could not be synthesized directly from 4-aminophenol and had to be synthesized by methyl ether cleavage of the dimethoxy derivative 6 with boron tribromide. In solution, the product is sensitive to oxidation and light and degraded rapidly on contact with silica gel. Coating of the flash column with ascorbic acid prevented degradation, and the pure compound was obtained. In its crystalline state, compound 7 is air-stable if stored in the dark at 0 °C.

Table 2. Inhibitory Activity of 4,5-Dianilinophthalimide Derivatives against Tyrosine and Serine Kinases


compd	R ₁	R ₂	R ₃	R ₄	R ₅	enzymatic activity IC ₅₀ (μM)				
						EGF-R ^a	<i>v-abl</i>	<i>c-src</i>	RKC	PKA
1	H	H	H	H		>100	nd	nd	>500	>500
2	F	F	H	H		>100	nd	nd	>500	>500
3	H	H	H	H	H	0.3	>50	16	80	>500
4	F	F	H	H	H	0.7	>50	50	32	>500
5	CH ₃	CH ₃	H	H	H	2.5	>100	>100	>100	>500
6	OCH ₃	OCH ₃	H	H	H	>50	>50	nd	460	>500
7	OH	OH	H	H	H	2.5	12	8	75	>500
8	N(C ₂ H ₅) ₂	N(C ₂ H ₅) ₂	H	H	H	50	>50	>100	>500	>500
9	I	I	H	H	H	>50	nd	nd	>500	>500
10	CN	CN	H	H	H	>100	nd	nd	>100	>500
11	C ₆ H ₅	C ₆ H ₅	H	H	H	>50	nd	nd	>500	>500
12	OCH ₃	H	H	H	H	2.0	>100	64	>100	>500
13	H	H	-CH ₂ CH ₂ -	H	H	>100	>50	>50	270	>500
14	H	H	CH ₃	H	H	8.7	>50	1.0	>500	>500
15	H	H	CH ₃	CH ₃	H	>50	>50	>100	>500	>500
16	H	H	COCH ₃	H	H	>50	>50	nd	>100	>500
17	H	H	H	H	C ₆ H ₅	>100	nd	nd	>100	>500
18	H	H	H	H	CH ₃	>50	nd	nd	>100	>500
19						>50	>50	>50	>100	>500
21						>100	nd	nd	>50	>500
staurosporine aglycon			H	H	H	>100	nd	nd	0.31	>10
dibisindolylmaleimide			H	H	H	>50	20	nd	0.19	200

^a Genistein was used as internal standard (IC₅₀ = 1 μM).

**Figure 1.** Comparison of dianilinophthalimide, staurosporine aglycons, and diindolylmaleimides.

The dicyano derivative 10 could not be obtained directly from 4-aminobenzonitrile and had to be synthesized from compound 9 by a Rosenmund-von Braun reaction.²⁴ Treatment of the diiodo derivative 9 with copper(I) cyanide in dimethylformamide at 140 °C produced compound 10 in low yields.

In order to obtain N(4),N(5)-substituted phthalimides 14–16, the dimethyl phthalate 1 was alkylated or acylated to compounds 2h–j which were then converted to the corresponding phthalimides by standard treatment with

ammonia gas in ethylene glycol. Methylation of 1 required harsh conditions (heating with potassium carbonate and with a large excess of iodomethane in dimethylformamide in a sealed tube) to give a mixture of 2h and 2i, which were separated by flash chromatography. Acetylation needed the same harsh conditions and produced the benzimidazolium chloride 2j, which was converted directly into the monoacetylphthalimide 16 by standard treatment with ammonia gas in ethylene glycol. The observed low nucleophilic potential of the N(4)- and N(5)-amino groups is in line with the observations made in the crystal structure. The pK_a of (the conjugated acids of) these two amino groups was measured to be ≤0.

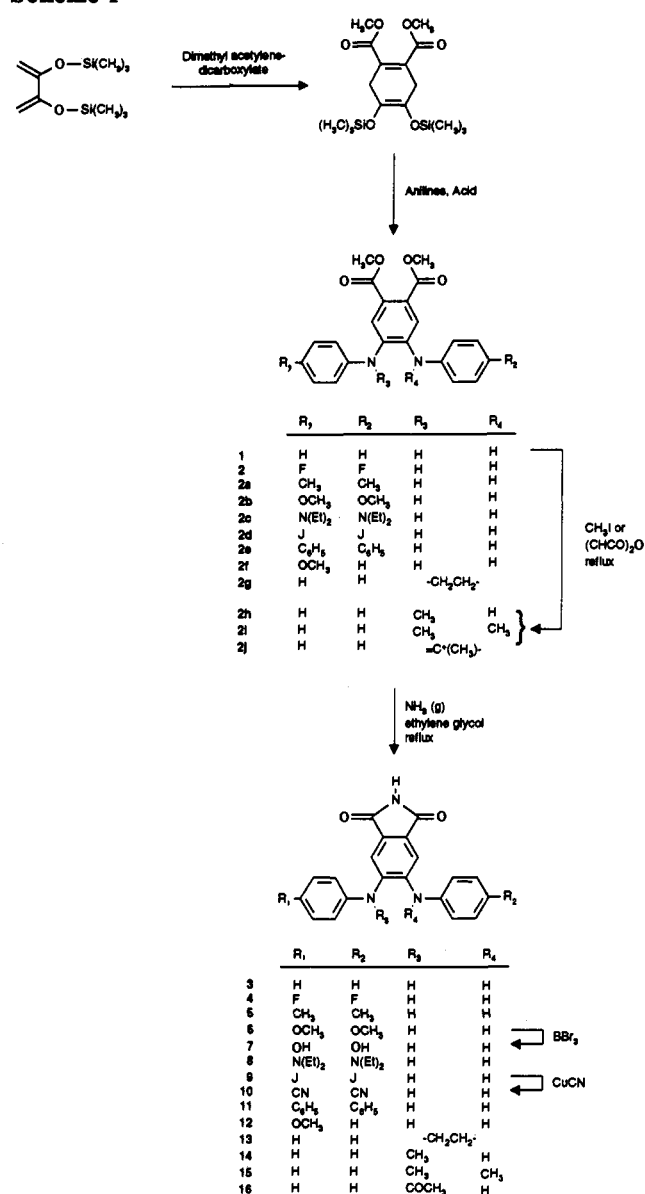
Dimethyl 4,5-bis(N-cyclohexylamino)phthalate 2k was formed by the reaction of dimethyl 4,5-bis((trimethylsilyloxy)cyclohexa-1,4-dienedicarboxylate with cyclohexylamine, which had to be present in a large excess in order to drive the reaction. Compound 2k was converted to the corresponding phthalimide 19 using standard treatment with ammonia gas in ethylene glycol (Scheme 3).

The thio analogues 20 and 21 had to be prepared by a different route because thiophenol did not react with dimethyl 4,5-bis((trimethylsilyloxy)cyclohexa-1,4-dienedicarboxylate under a variety of conditions (data not shown). Diels–Alder reaction of maleimide with the easily accessible 3,4-bis(phenylthio)sulfolene^{25,26} formed the tetrahydrophthalimide 20 in good yields, which was dehydrogenated to the phthalimide 21 with DDQ in refluxing toluene with low yield (Scheme 4).

Biological Evaluation and Discussion

Enzymatic Activity. Compounds were tested against a panel of tyrosine and serine/threonine kinases (Table

Scheme 1



2). The most active compounds 3–5 and 12 of this series showed IC_{50} values between 0.3 and 2.5 μM for the inhibition of the tyrosine kinase activity of a recombinant EGF-R (EGF-R ICD).²⁷ When tested for selectivity against the *v-abl* and *c-src* tyrosine kinases, no or only marginal inhibition was found for all compounds with the exception of the 4,4'-dihydroxy derivative 7 (which showed no selectivity) and the *N*-methyl derivative 14 which showed IC_{50} values of 1 and 8 μM , respectively, against the *c-src* kinase. In addition, when tested against serine/threonine kinases, only marginal inhibition of PKC (mixture of isozymes, purified from porcine brain) was found for compound 3 ($\text{IC}_{50} = 80 \mu\text{M}$), compound 4 ($\text{IC}_{50} = 32 \mu\text{M}$), and compound 7 ($\text{IC}_{50} = 75 \mu\text{M}$), whereas all the compounds of this series were inactive against PKA (IC_{50} values $>500 \mu\text{M}$).

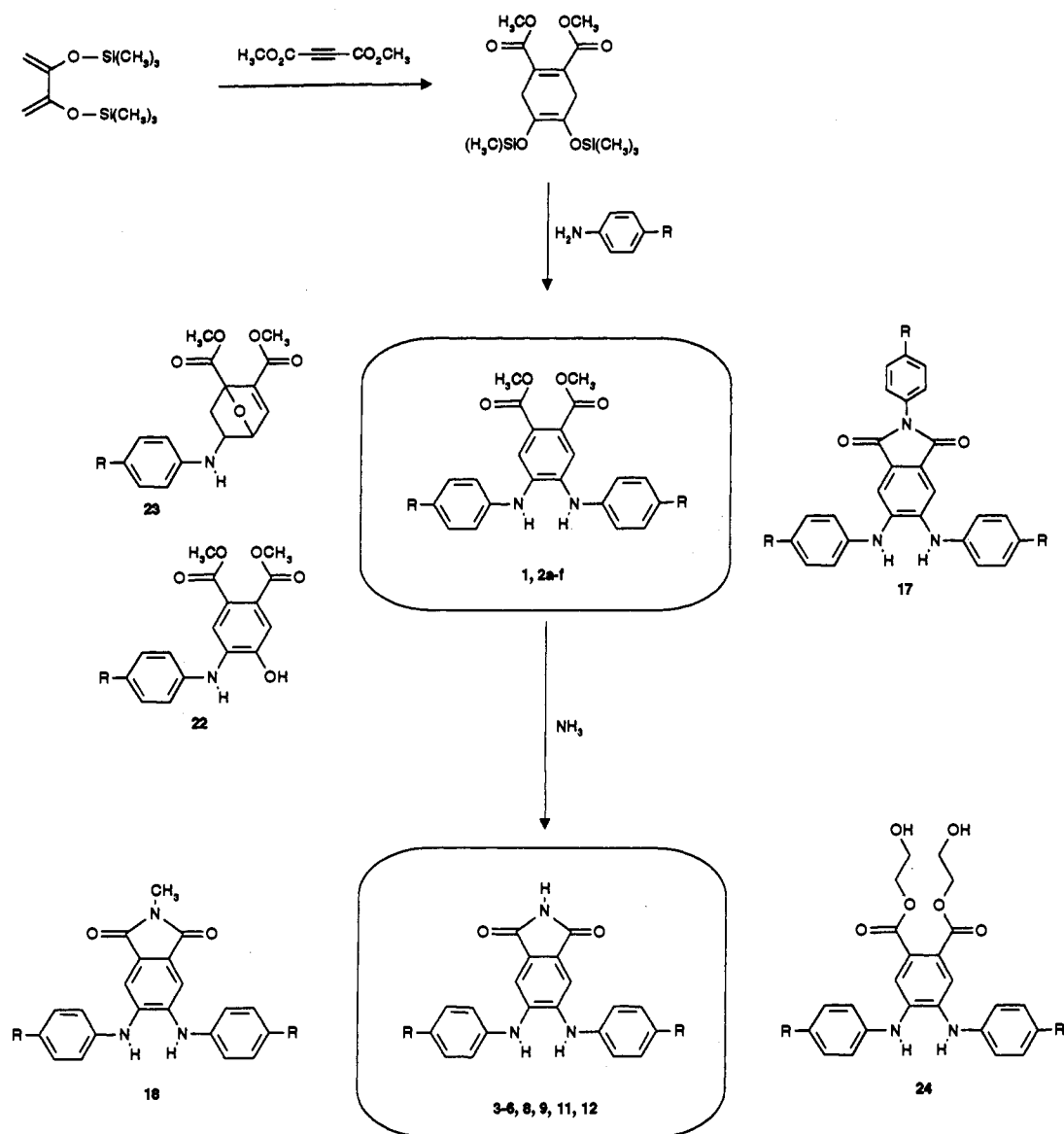
The following structural motifs have been found to be important for inhibition of activity against the EGF-R tyrosine kinase (Table 2). (1) A free phthalimide nitrogen: Substitution of hydrogen at position R₅ completely abolished inhibition (compounds 17 and 18); compounds 1 and 2, two synthetic precursors of compounds 3 and 4, respectively, were also inactive. (2) Intact phenyl rings:

The cyclohexyl analogue 19 was inactive. (3) Small substituents at both aniline rings: Only fluorine in R₁ and R₂ retained activity (compound 4); bulkier substituents like methoxy (compound 6), diethylamino (compound 8), iodine (compound 9), but also the relatively small cyano group (compound 10), at the same positions abolished activity. (4) Free diphenylamine nitrogen: Substitution at R₃ and R₄ greatly decreased inhibition (compound 13 and 14) or abolished it (compounds 15 and 16). Replacement of the aniline function by a thiophenyl moiety again completely abolished inhibition (compound 21).

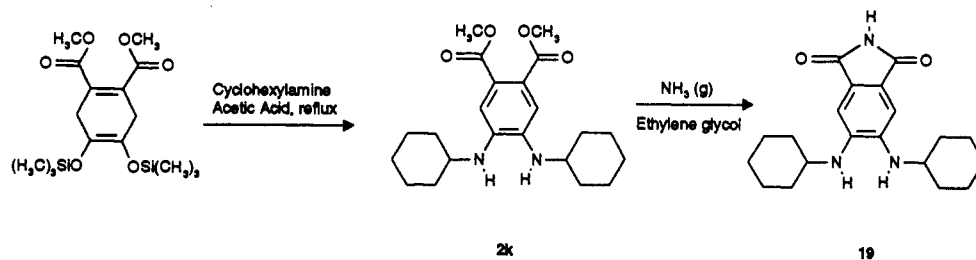
Competition experiments with compound 3 were performed and analyzed according to Eadie-Hofstee to determine the kinetic nature of inhibition relative to ATP and phospho-acceptor peptide (Figure 2). Compound 3 showed competitive type inhibition against ATP ($K_i = 0.16 \mu\text{M}$).

As already mentioned, 4,5-dianilinophthalimides are structurally closely related to the staurosporine aglycons and to diindolylmaleimides, which are potent ATP-competitive PKC inhibitors devoid of activity against the EGF-R tyrosine kinase. ATP, the cofactor for all protein kinases, has reported K_m values between 2 and 20 μM .^{28–32} Even though ATP is not very tightly bound, protein kinases exert a high degree of selectivity for adenine nucleotides vs other nucleotides. The K_m value for GTP is usually a factor of 20–100 times higher, and the pyrimidine nucleoside triphosphates have K_m values of a factor of 500 higher than ATP.^{28–32} Sequence alignments have shown that certain amino acids within the ATP binding site are highly conserved among all protein kinases.³³ This led to the idea that ATP-competitive inhibitors would lack selectivity. The reversal of the selectivity profile, seen between staurosporine aglycons and 4,5-dianilinophthalimides, was therefore unexpected and might be explained by the conformation of compound 3 shown in the crystal structure (Figure 3). Even though the molecular structure suggests a highly symmetric molecule, the crystal structure of compound 3 revealed an asymmetric propeller-shape conformation, which is probably due to a subtle balance of steric and electronic factors. It should be noted that the hydrogen atoms at the 3- and 6-position of the phthalimide ring and the 2'-hydrogens of the aniline rings are at distances of 2.3 and 2.4 Å, which are close to their contact distances. The distance between the two amino hydrogens is 2.0 Å, which is equal to the sum of their van der Waals radii. From force field calculations, there is little doubt that this conformation represents the energy minimum. In contrast to compound 3, staurosporine aglycons are planar molecules³⁴ and diindolylmaleimides show a bowl-shaped conformation.²² We believe that this conformational difference between dianilinophthalimides and staurosporine aglycons or diindolylmaleimides is responsible for the different selectivity profile with respect to inhibition of protein kinases. Despite of the sequence homology in the ATP binding regions among serine/threonine and tyrosine kinases,³³ these results show that ATP-competitive compounds have the potential to be potent and selective inhibitors of protein kinases. This can be rationalized in view of the fact that ATP is relatively weakly bound and that minor amino acid substitutions in the ATP binding pocket at positions not involved in ATP binding could alter the enzyme surface and therefore the affinity for inhibitor molecules.

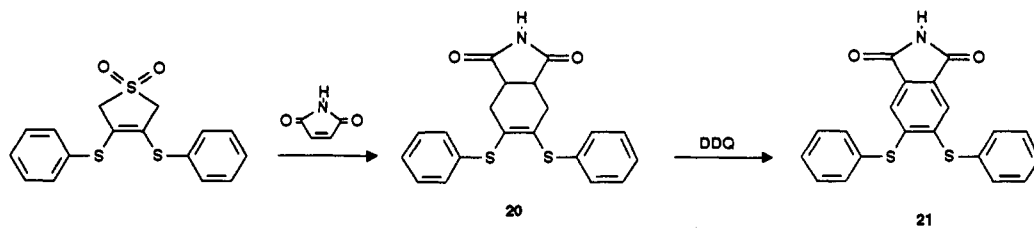
Scheme 2



Scheme 3



Scheme 4



Cellular Activity. Investigations of the intracellular pathways by which extracellular stimuli activate cellular proliferation have shown that ligand binding to receptor type protein tyrosine kinases (e.g. EGF-R and platelet-

derived growth factor receptor (PDGF-R)) triggers a cascade of biochemical events. Autophosphorylation of the C-terminus of the EGF-R is considered to be the first enzymatic event following ligand binding.^{35,36} C-terminal

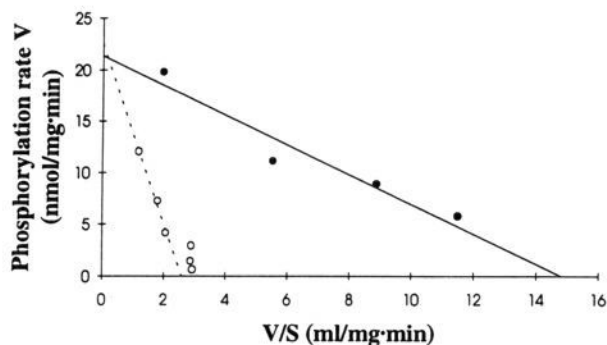


Figure 2. Kinetics of inhibition of the EGF-R ICD kinase by compound 3. Steady-state kinetic analysis was performed in the absence (●) or presence (○) of 1 μ M compound 3, using 200 ng of EGF-R ICD kinase, 20 mM Tris-HCl, pH 7.5, 10 mM MnCl₂, 2 mM angiotensin II, and varying concentrations of ATP (0.2–10 μ M). Assays were performed at 20 °C for 10 min. Apparent kinetic constants were calculated from Eady-Hofstee plots after linear regression of the experimental data. For K_i determination, inhibitor was used at the IC_{50} concentration and the nonvaried substrate at $1 \times K_m$.

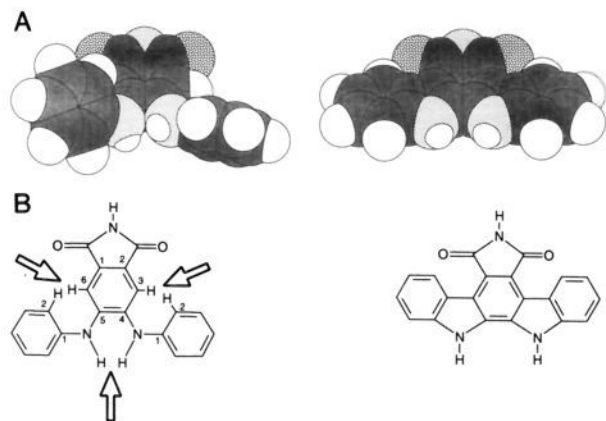


Figure 3. Crystal structure of compound 3 and staurosporine aglycon. The X-ray structure of compound 3 and that of the staurosporine aglycon are shown in the space-filling and the ball-and-stick model (panel A). Compound 3 shows a propeller-shaped conformation while the staurosporine aglycon is flat. It should be noted that the hydrogen atoms at the 3- and 6-positions of the phthalimide ring and the 2'-hydrogens of the aniline rings are at a distance of 2.3 and 2.4 Å, which is close to the minimal possible distance. The distance between the two amino hydrogens is 2.0 Å, which is equal to the sum of their van der Waals radii. The positions of these atoms are outlined in red in the formula of compound 3 (panel B).

autophosphorylation sites are physiological target substrates of the EGF-R kinase *in vivo*.³⁷ The physiological role of this event is incompletely understood but is generally considered to be a regulatory mechanism which is required for enzyme activation^{38,39} and for SH2 (src-homology region 2)-mediated protein-protein interactions.⁴⁰ A further event which is initiated early in the action of such growth factors is the transcription of "immediate early response genes" such as the proto-oncogene *c-fos*. Induction of these genes is essential for the initiation of cellular events which are required for cell replication. The expression of *c-fos* mRNA can rapidly and transiently be induced by a variety of extracellular stimuli acting via a number of second-messenger pathways.^{41,42} Thus, monitoring both the modulation of receptor autophosphorylation and the levels of expression of *c-fos* mRNA offers a convenient method to study the mode of action and selectivity of protein kinase inhibitors.

We have used these molecular markers to analyze the selectivity of dianilino-phthalimides for their inhibition of EGF-mediated signal transduction in the cell.

Selective Inhibition of EGF-Induced Tyrosine Phosphorylation in Intact Cells. A specific set of intracellular proteins, including the EGF-R itself, are phosphorylated on tyrosine residues in response to EGF.^{35,36} A novel ELISA was used to measure the effects of active compounds 3–5 and 12 on EGF-stimulated cellular tyrosine phosphorylation in the A431 human epithelial carcinoma cell line (which is known to express high levels of EGF-receptor).^{43,44} Inactive compounds 6, 11, 14, and 16–18 were used as negative controls. As shown in Table 3, the *in vitro* active compounds 3–5 and 12 inhibited EGF-stimulated cellular tyrosine phosphorylation. With compounds 3–5 and 12, a good correlation between the IC_{50} values for the inhibition of EGF-stimulated cellular tyrosine phosphorylation and *in vitro* enzyme inhibition was found. As expected, none of the derivatives 6, 11, 14, and 16–18, which were inactive at the enzyme level, showed inhibition of EGF-dependent cellular tyrosine phosphorylation.

These results were confirmed in an additional cellular autophosphorylation assay by western blotting using anti-phosphotyrosine antibodies.⁴⁵ In this assay, EGF stimulation resulted in tyrosine phosphorylation of a protein with a molecular weight of 180 000 (Figure 4, lane 2). Pretreatment of the cells with compound 3 or 4 caused a concentration-dependent inhibition of ligand-stimulated EGF-R autophosphorylation, with an estimated IC_{50} value between 1–10 μ M (Figure 4, lanes 3–5 and 7–10). Overall levels of the EGF-receptor were not affected by these compounds (data not shown). In order to define the specificity of the compounds, we tested their effects on PDGF-stimulated tyrosine phosphorylation in BALB/c 3T3 fibroblasts, which express high levels of the PDGF-R. PDGF-induced tyrosine phosphorylation was not inhibited up to a concentration of 100 μ M by compounds 3–6, 11, 12, 16–18 (Table 3). Compound 14 inhibited PDGF-induced tyrosine phosphorylation with an IC_{50} of 12 μ M. Identical results were obtained by western blotting (data not shown).

Selective Inhibition of EGF-Induced *c-fos* mRNA Expression. Stimulation of quiescent BALB/c 3T3 cells by EGF, PDGF, or fibroblast growth factor (FGF) rapidly induces the expression of *c-fos* mRNA.^{41,42} Pretreatment of the cells with compound 3 or 4 for 90 min prior to stimulation with EGF strongly inhibited *c-fos* expression with an IC_{50} of 3–10 μ M (Figure 5, panels A and B, lanes 3–7) which is similar to the value determined for the inhibition of EGF-R autophosphorylation. In contrast, expression of the *c-fos* gene induced by ligand-stimulated PDGF- and FGF-receptor activation was reduced only at 30–100 μ M concentration with both compounds (data not shown).

Antiproliferative Activity. Selected compounds were tested for their antiproliferative activity in a 5-day proliferation assay using BALB/MK mouse epidermal keratinocytes, which are dependent on EGF.⁴⁶ As shown in Table 3, compounds which were potent EGF-R protein tyrosine kinase inhibitors at the enzyme level (compounds 3–5 and 12) also showed potent antiproliferative activity, whereas derivatives which were inactive at the enzyme level (compounds 6, 11, 14, and 16–18) showed no or only marginal antiproliferative activity.

Table 3. Cellular Activity of 4,5-Dianilinophthalimide Derivatives

3-18

compd	R ₁	R ₂	R ₃	R ₄	R ₅	cellular activity IC ₅₀ (μM)		
						inhibition of EGF-dependent autophosphorylation A431-carcinoma	inhibition of PDGF-dependent autophosphorylation Balb/3T3 fibroblasts	antiproliferative activity Balb/MK cells
3	H	H	H	H	H	4.5	100	11.5
4	F	F	H	H	H	2.2	100	8.5
5	CH ₃	CH ₃	H	H	H	4.5	>100	9.3
6	OCH ₃	OCH ₃	H	H	H	>100	>100	18.5
11	C ₆ H ₅	C ₆ H ₅	H	H	H	>100	>100	>50
12	OCH ₃	H	H	H	H	18	>100	11.4
14	H	H	CH ₃	H	H	>100	12	34.3
16	H	H	COCH ₃	H	H	>50	>100	>50
17	H	H	H	H	C ₆ H ₅	>50	>100	>50
18	H	H	H	H	CH ₃	>50	>100	20.6

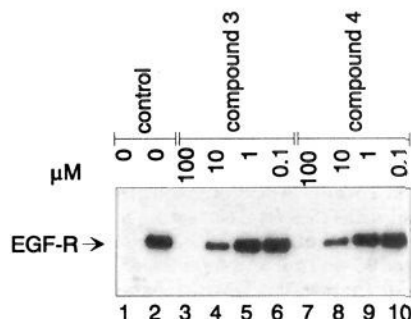


Figure 4. Selective Inhibition of EGF-R in intact cells. Serum-starved A431 cells were incubated for 90 min with the indicated concentrations of compounds 3 (lanes 3–6) or compound 4 (lanes 7–10) prior to stimulation with EGF (100 ng/mL; lanes 2–10) for 10 min, respectively. Equal amounts of protein of cell lysates were analyzed by western blotting using antiphosphotyrosine antibodies.⁵²

These cellular results indicate that dianilinophthalimide derivatives, especially compounds 3 and 4, show high selectivity for inhibition of “early events” in signal transduction via ligand-activated EGF-R. The high cellular activity of this class of inhibitors is likely due to their lipophilic nature, which should aid cellular penetration.

In Vivo Antitumor Activity. The antitumor activity of compound 3 has been tested *in vivo* (submitted for publication⁴⁷) against xenografts of the A431 and SK-OV-3 tumors, which overexpress the EGF receptor and p185^{c-erbB2}, respectively. Compound 3 showed significant tumor growth inhibition. A clear dose response was seen with maximum response achieved between 25 and 50 mg/kg. Doses as low as 6.3 mg/kg (1/80 MTD) still showed antitumor effects, while only marginal effects were seen at 3.2 mg/kg. In contrast, a PDGF driven tumor was not inhibited by compound 3 (submitted for publication, ref 47), which is compatible with its cellular selectivity and hypothesized mechanism of action. No overt cumulative toxicity was observed during treatment even though high efficacy was observed, indicating a good therapeutic window.

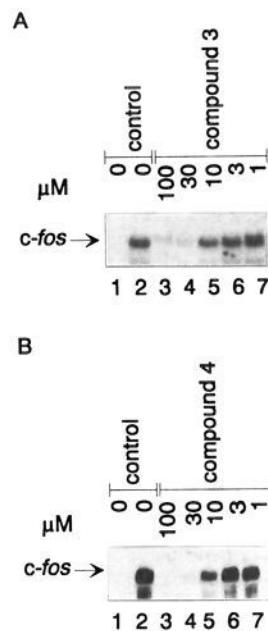


Figure 5. Effect of compounds 3 and 4 on *c-fos* mRNA expression. Confluent, quiescent BALB/c 3T3 cells were incubated for 90 min with the indicated concentrations of compound 3 (panel A, lanes 3–7) or 4 (panel B, lanes 3–7). After stimulation with EGF (20 ng/mL, lanes 2–7) for 30 min, samples of total RNA⁵⁵ were analyzed by the northern blot technique using a digoxigenin-labeled SP6 RNA probe complementary to the 1.3 kb Bgl II/Pvu II fragment of the *v-fos* cDNA.⁵⁶ Digoxigenin-labeled probe was detected by using anti-digoxigenin Fab fragment conjugated alkaline phosphatase and the chemiluminescent substrate AMPPD. Equal loading of RNA was verified by staining of the gels with ethidium bromide.

In summary, 4,5-dianilinophthalimides represent a novel class of inhibitors of the EGF-R family of protein tyrosine kinases with high selectivity and potency at the enzymatic and the cellular level. They are efficiently taken up by cells and show selectivity for inhibition of the EGF-driven signal transduction pathway. Compound 3 has antitumor activity *in vivo* at well-tolerated doses. This class of

compounds offers potential candidates for further development and clinical evaluation.

Experimental Section

Materials and Methods. The peptides angiotensin II, [Val⁵]-angiotensin II, kemptide, and random polymer Glu,Tyr (4:1) were from Sigma (St. Louis, MO). PMA (phorbol 12-myristate 13-acetate) and *p*-nitrophenyl phosphate were from Fluka (Buchs, CH). Leupeptin and aprotinin were from Boehringer (Mannheim, Germany). [γ -³²P]ATP was from Amersham (Amersham, U.K.). Monoclonal antiphosphotyrosine hybridoma 4G10⁴⁶ was provided by Dr. T. Roberts (Dana Faber Cancer Inst., Boston, MA). Rabbit polyclonal antibodies directed against the EGF-R were obtained from Cambridge Research Biochemicals (Cambridge, U.K.). PKA from rabbit muscle was a gift from Dr. B. Hemmings, Friedrich Mischer Inst. (Basel, Switzerland). A431 human squamous carcinoma cells were obtained from the European Collection of Animal Cell Cultures (ECACC, Porton Down, UK). The EGF-dependent BALB/MK mouse keratinocyte cell line was kindly provided by Dr. S. Aaronson.⁴⁶ Female BALB/c nude mice were obtained from Bømhøltgard (Denmark). Vecstatin ABC-AP kit and alkaline phosphatase substrates were obtained from Vector Laboratories (Burlingame, CA). EGF was obtained from Biomedical Technologies Inc. (Stoughton, MA) and bovine calf serum was from Hyclone (Logan, UT). Human PDGF (platelet-derived growth factor) B-chain was from Bissendorf Biochemicals (Hannover, Germany), and bFGF, cell culture reagents, and materials were from Gibco (Paisley, UK). Sodium orthovanadate was from Fisher Chemicals. Immobilon-P membranes were from Millipore (Bedford, MA), and glass fiber filter papers and P81 paper were obtained from Whatman (Maidstone, UK).

Preparation of Enzymes. The intracellular domain of the EGF-R (EGF-R ICD) and *c-src* kinases were expressed in Sf9 cells using recombinant baculoviruses and purified as previously described.^{27,48} The specific activities of EGF-R ICD and *c-src*, measured at 20 °C using 10 μ M ATP and random polymer poly Glu,Tyr as substrate, were 20 nmol/(min/mg) and 120 nmol/(min/mg), respectively. Recombinant *v-abl* kinase was expressed in *E. coli* using vector *p-ablHP*. The fusion protein *A/abl* product encoded by this vector was affinity purified on IgG-Affigel 10 as previously described.⁴⁹ The specific activity of *v-abl*, assayed at 20 °C in the presence of 10 mM MgCl₂ with [Val⁵]angiotensin II as substrate, was 1.5 nmol/(min/mg). Protein kinase C (PKC) from porcine brain and cyclic AMP-dependent protein kinase (PKA) were prepared as previously described.¹⁵ Activity determinations of PKC using histone H1 (0.2 mg/mL) as substrate, and of PKA using kemptide (0.1 mg/mL) as substrate, were performed as described previously.¹⁵

Kinase Assays. Determination of EGF-R ICD kinase activity was performed as described²⁷ using angiotensin II as substrate. All compounds were dissolved in DMSO, giving a final concentration of 1% in the assay. Genistein (IC₅₀ = 1 μ M) served as an internal standard inhibitor in all assays.

c-src tyrosine protein kinase activity was assayed using polymer poly(Glu,Tyr) as phosphate acceptor substrate. The reaction mixtures (50 μ L) contained 20 mM Tris-HCl pH 7.5, 10 mM MgCl₂, 1 mM dithiothreitol, 20 μ M [γ -³²P]ATP (approximately 30 Ci/mol), 10 ng of enzyme protein and 25 μ g/mL polymeric substrate. Reactions were carried out at 20 °C for 10–15 min and terminated by adding 10 μ L of ice-cold 0.5% H₃PO₄. Aliquots of the reaction mixture were spotted onto P81 paper and processed as previously described.^{15,50}

v-abl kinase was assayed as previously described⁵⁰ using 1 mM [Val⁵]angiotensin II and 10 μ M [γ -³²P]ATP (0.33 Ci/mmol) as substrates.

Enzyme Kinetics. Substrate kinetics were performed by adding the nonvariable substrate at 2 \times K_m concentration. Apparent kinetic constants were calculated from Eady-Hofstee plots after linear regression of the experimental data. For K_i determination, inhibitor was used at the IC₅₀ concentration and the nonvaried substrate at 1 \times K_m.

Cell Culture Conditions. BALB/MK mouse epidermal keratinocytes were grown in calcium-free DMEM and HAM's F12 medium (1:1, v/v), supplemented with 5% fetal calf serum and EGF (5 ng/mL).

BALB/c 3T3 cells were grown in DMEM supplemented with 10% calf serum. Quiescent cultures were obtained by growing cells for 5–7 days without medium change. Cells were washed, and DMEM containing 1 mg/mL bovine serum albumin was added during treatment with drug and mitogen.

A431 human epithelial carcinoma cells were cultured in DMEM supplemented with 10% fetal calf serum. Cells were grown to 80% confluency and then starved in DMEM containing 0.5% fetal calf serum for 24 h. Compound in 1% DMSO (final concentration) was added 90 min prior to stimulation with EGF.

Preparation of Cell Extracts. Following treatment, cells were washed with ice-cold phosphate-buffered saline (PBS) containing 200 μ M sodium orthovanadate and lysed in 0.8 mL of lysis buffer (50 mM Tris-HCl, pH 7.5, 5 mM EGTA, 1% Triton X-100, 150 mM NaCl, 1 mM phenylmethane sulfonyl fluoride, 80 μ g/mL aprotinin, 50 μ g/mL leupeptin, 200 μ M sodium orthovanadate) at 4 °C for 10 min. Lysates were cleared by 10 min centrifugation at 10 000g and were adjusted to equal protein content. Protein determination was carried out according to the method of Bradford.⁵¹

Western Blotting. Cell extracts were separated by SDS-PAGE (7.5% acrylamide) and transferred to Immobilon-P membranes by semidry blotting. Membranes were blocked and then incubated with mouse monoclonal antibodies against phosphotyrosine overnight at 4 °C. EGF-R expression was monitored in a similar manner using EGF-R specific rabbit antiserum. After washing, bound antibodies were detected using the Immun-lite assay kit from BIORAD.

Inhibition of Cellular Tyrosine Phosphorylation in A431 Cells. A microtiter ELISA assay method was developed for the determination of the IC₅₀ values of compounds for inhibition of EGF- or PDGF-stimulated cellular tyrosine phosphorylation. 2 \times 10⁴ A431 cells were plated per well of a 96-well microtiter plate and incubated for 3 days or until the cultures reached confluency at 37 °C, 7.5% CO₂. Cell monolayers were then washed twice with PBS and covered with 200 μ L of fresh culture medium supplemented with 0.5% fetal calf serum for 24 h. BALB/c 3T3 cells were grown to confluency within 3–5 days after plating on collagen-coated 96-well microtiter plates without medium change. After removal of the medium, DMEM containing 1 mg/mL bovine serum albumin was added. Test compounds were added in serial dilutions for 2 h prior to growth factor stimulation. EGF or PDGF was added at a final concentration of 100 ng/mL or 50 ng/mL, respectively, and incubated for 10 min. Culture medium was removed, and cells were washed with PBS and fixed for 10 min with methanol (–20 °C). Subsequently, blocking solution (3% BSA in PBS, 0.2% Tween 20, normal horse serum for anti P-Tyr antibody) was added for 1 h at 37 °C. Primary antibodies were diluted in 3% BSA containing 0.05% NaN₃. Mouse monoclonal antibody 4G10⁵² directed against phosphotyrosine was diluted 1:3 \times 10⁴ before use. Incubation with primary antibody was done for 1 h at 37 °C. Development of the plates was performed using a Vecstatin ABC-AP kit using *p*-nitrophenyl phosphate as the substrate. Plates were developed in the dark for 20 min and read at 405 nm. Plates included wells without growth factor and compound, without compound and control wells lacking the primary antibody. In a typical experiment, addition of EGF or PDGF gave rise in OD₄₀₅ by a factor of 4 over unstimulated cells. IC₅₀ values are defined as the drug concentrations leading to a 50% inhibition of the EGF- or PDGF-stimulated increase in cellular phosphotyrosine.

Antiproliferative Assays. Assays were performed essentially as previously described.¹⁵ Cells (BALB/MK) (10⁴/well) were seeded into 96-well microtiter plates and incubated overnight. Drugs, dissolved in DMSO, were added in serial dilutions (the final DMSO concentration in all assays was 1%). After addition, the plates were incubated for 5 days, which allowed control cultures to undergo at least three cell divisions. Growth of MK cells was monitored using methylene blue staining. IC₅₀ values were defined as the drug concentrations that resulted in a 50% decrease in cell number as compared to the control cultures in the absence of inhibitor. IC₅₀ values represent the mean and standard deviations of three independent experiments.

In Vivo Antitumor Activity. Procedures for determination of maximal tolerated dose (MTD) were as described previously.¹⁵ Antitumor activity was tested using the human epidermoid

carcinoma A431 (ATCC No. CRL 1555). Pieces of solid tumor were transplanted to the left flank of female BALB/c nude mice. The treatment was started on day 8 or 11 after tumor transplantation when the tumors reached a diameter of 5–6 mm. Compounds were administered orally once daily for 14 days. Tumor growth was followed by measuring perpendicular tumor diameters. Tumor values were calculated as previously described.⁶³ Drug solutions were prepared in 100% ethanol (40 mg/mL), containing 1 drop of Tween 80/mL, and heated at 40 °C until a clear solution was obtained. Stock solution was diluted 1:20 (v/v) with 0.9% NaCl and used for treatment. Fresh solution were prepared before each treatment.

Synthesis. Melting points were determined in open capillary tubes and are uncorrected. High-performance liquid chromatography was performed using a Kontron MT 450 apparatus with UV detection at 254 nm. Elemental analyses were within $\pm 4\%$ of the theoretical value. UV/vis spectra were obtained with a Perkin-Elmer Lambda 9 spectrophotometer. Infrared spectra were recorded on a Perkin-Elmer 1310 or 298 spectrophotometer. ¹H NMR and ¹³C NMR were recorded on a Varian Gemini 200, a Varian Gemini 300, or a Bruker WM-360 spectrometer. The coupling constants are recorded in hertz (Hz), and the chemical shifts are reported in parts per million (δ , ppm) downfield from tetramethylsilane (TMS). Mass spectra (MS), fast-atom-bombardment mass spectra (FABMS), and high-resolution mass spectra (HRMS) were recorded on a VG Manchester apparatus. Analytical thin-layer chromatography (TLC) was carried out on precoated plates (silica gel, 60 F-254, Merck), and spots were visualized with UV light, iodine, or phosphormolybdate. Column chromatography was performed with Kieselgel 60 (230–400 mesh) silica gel (Merck). Removal of solvents was performed by rotary evaporation under reduced pressure. All reactions involving air- or moisture-sensitive reagents were performed under a positive pressure of argon. Organic solvents were purified by the methods described by D. D. Perrin, W. L. F. Armarego, and D. R. Perrin (*Purification of Laboratory Chemicals*; Pergamon: Oxford 1986) or were purchased reagent grade from Aldrich or Fluka. Starting materials were purchased from Fluka or Aldrich. Bis(phenylthio)sulfolene was synthesized starting from 3-sulfolene in four steps in 17% overall yield by the method of Chou et al.²⁵ Dimethyl 4,5-bis((trimethylsilyloxy)cyclohexa-1,4-dienedicarboxylate was synthesized starting from diacetyl in two steps in 52% overall yield by the method of Matlin et al.²³

Dimethyl 4,5-dianilinophthalate (1). **General Method A.** A solution of dimethyl 4,5-bis((trimethylsilyloxy)cyclohexa-1,4-dienedicarboxylate (2.24 g, 6 mmol) and aniline (2.2 mL, 24 mmol) in glacial acetic acid (24 mL) was stirred at reflux (3 h). The reaction mixture was cooled to room temperature and taken to dryness. The dark brown residue was dissolved in dichloromethane and washed with 1 N HCl, saturated NaHCO₃, and water. The organic phase was dried with sodium sulfate, filtered, and taken to dryness. Crystallization from boiling ethanol yielded pure 1 as yellow crystals (823 mg, 36%): mp 177–180 °C; TLC (dichloromethane/methanol, 98:2) *R_f* 0.75 (UV); ¹H NMR (CDCl₃) δ 7.53 (s, 2H), 7.30 (t, 4H, *J* = 7.5 Hz), 7.00 (t, 2H, *J* = 7.5 Hz), 6.98 (d, *H*, *J* = 7.5 Hz), 5.84 (br s, 2H), 3.85 (s, 6H); IR (CH₂Cl₂) ν_{\max} 3370, 1720, 1600, 1575, 1500, 1340, 1290–1240, 1220, 1140; FABMS *m/z* 377 (M⁺ + H). Anal. (C₂₂H₂₀N₂O₄) C, H, N.

Dimethyl 4,5-Bis(4-fluoroanilino)phthalate (2). Compound 2 was prepared from 4-fluoroaniline in 37% yield using method A. The raw product was flash chromatographed on silica gel using hexanes/ethyl acetate (1:2) as eluent, and the product fractions were taken to dryness and crystallized from ethyl acetate/hexanes to yield pure 2 as yellow crystals: mp 164–166 °C; TLC (hexanes/ethyl acetate, 1:1) *R_f* 0.66 (UV); ¹H NMR (CDCl₃) δ 7.39 (s, 2H), 7.09–6.85 (m, 9H), 5.72 (br s, 2H), 3.81 (s, 6H); FABMS *m/z* 413 (M⁺ + H), 412 (M⁺). Anal. (C₂₂H₁₈F₂N₂O₄) C, H, N.

Dimethyl 4,5-Bis(4-methylanilino)phthalate (2a). Compound 2a was prepared from 4-methylaniline in 24% yield using method A as yellow crystals: mp 170–172 °C; TLC (hexanes/ethyl acetate, 2:1) *R_f* 0.48 (UV); ¹H NMR (CDCl₃) δ 7.55 (br s, 2H), 7.30 (s, 2H), 7.13/7.00 (AB, 8H, *J* = 9.0 Hz), 3.70 (s, 6H), 2.25 (s, 6H); MS *m/z* 404 (M⁺).

Dimethyl 4,5-Bis(4-methoxyanilino)phthalate (2b). Compound 2b was prepared from *p*-anisidine in 41% yield using

method A. The raw product was flash chromatographed on silicagel with hexanes/ethyl acetate (1:1) as eluent, and the product fractions were taken to dryness to yield pure 2b as yellow foam: TLC (hexanes/ethyl acetate, 1:1) *R_f* 0.5 (UV); ¹H NMR (CDCl₃) δ 7.33 (s, 2H), 6.95/6.85 (AB, 8H, *J* = 9.5 Hz), 5.60 (br s, 2H), 3.80 (s, 6H), 3.78 (s, 6H).

Dimethyl 4,5-Bis[4-(*N,N*-diethylamino)anilino]phthalate (2c). Compound 2c was prepared from 4-(*N,N*-diethylamino)aniline in 36.4% yield using method A. The raw product was flash chromatographed on silica gel using dichloromethane/methanol (400:15) as eluent. The product fractions were combined and flash chromatographed on silica gel using hexanes/ethyl acetate (1:1) as eluent, and the product fractions were taken to dryness and crystallized from ethyl acetate/hexanes to yield pure 2c as green crystals: TLC (hexanes/ethyl acetate, 1:1) *R_f* 0.44 (UV); ¹H NMR (CDCl₃) δ 7.29 (s, 2H), 6.92 (1/2 AB, 4H, *J* = 10 Hz), 6.78 (1/2 AB, 4H, *J* = 10 Hz), 5.49 (br s, 2H), 3.82 (s, 6H), 3.33 (q, 8H, *J* = 6.0 Hz), 1.17 (t, 12H, *J* = 6.0 Hz).

Dimethyl 4,5-Bis(4-iodoanilino)phthalate (2d). Compound 2d was prepared from 4-iodoaniline in 35% yield using method A and crystallized from ethyl acetate/hexanes to yield pale yellow crystals: TLC (hexanes/ethyl acetate, 1:1) *R_f* 0.7 (UV); ¹H NMR (DMSO-*d*₆) δ 8.00 (br s, 2H), 7.57 (1/2 AB, 4H, *J* = 9.5 Hz), 7.42 (s, 2H), 6.90 (1/2 AB, 4H, *J* = 9.5 Hz), 3.85 (s, 6H); FABMS *m/z* 629 (M⁺ + H).

Dimethyl 4,5-Bis(4-phenylanilino)phthalate (2e). Compound 2e was prepared from 4-aminobiphenyl in 39% yield using method A. The raw product was filtered through silica gel with dichloromethane as eluent, and the product fractions were taken to dryness and crystallized from boiling ethanol to yield pure 2e as yellow crystals: mp 196–197 °C; TLC (hexanes/ethyl acetate, 1:1) *R_f* 0.5 (UV); ¹H NMR (CDCl₃) δ 7.70–7.25 (m, 16H), 7.18 (d, 2H, *J* = 7.5 Hz), 5.90 (br s, 2H), 3.87 (s, 6H). Anal. (C₃₄H₂₈N₂O₄ · 1/2 H₂O) C, H, N.

Dimethyl 4-(Methoxyanilino)-5-anilinophthalate (2f). Compound 2f was prepared from a 1:1 mixture of 4-methoxyaniline and aniline in 14.5% yield using method A. The raw product was flash chromatographed on silica gel using hexanes/ethyl acetate (2:1) as eluent, eluting first compound 1, then compound 2f followed by compound 2b. The product fractions were combined and again flash chromatographed on silica gel using hexanes/ethyl acetate (3:2) as eluent, and the product fractions were taken to dryness and crystallized from ethyl acetate/hexanes to yield pure 2f as slightly greenish crystals: mp 118–120 °C; TLC (hexanes/ethyl acetate, 2:1) *R_f* 0.66 (UV); ¹H NMR (CDCl₃) δ 7.62 (s, 1H), 7.28 (t, 2H, *J* = 8 Hz), 7.20 (s, 1H), 7.02 (1/2 AB, 2H, *J* = 10 Hz), 6.92 (t, 1H, *J* = 8 Hz), 6.88 (d, 2H, *J* = 8 Hz), 6.87 (1/2 AB, 2H, *J* = 10 Hz), 5.95 (br s, 1H), 5.50 (br s, 1H), 3.85 (s, 3H), 3.82 (s, 3H), 3.81 (s, 3H); FABMS *m/z* 407 (M⁺ + H). Anal. (C₂₃H₂₂N₂O₅) C, H, N.

Compound 1 and compound 2b were obtained in 5% and 12% yield, respectively.

Diethyl 5,8-Diphenyl-5,8-diaza-5,6,7,8-tetrahydronaphthalene-2,3-dicarboxylate (2g). Compound 2g was prepared from 1,2-dianilinoethane in 28% yield using method A. The raw product was flash chromatographed on silica gel with hexanes/ethyl acetate (3:1) as eluent, and the product fractions were taken to dryness and crystallized from boiling ethanol to yield pure 2g as orange crystals: mp 146–148 °C; TLC (dichloromethane) *R_f* 0.32 (UV); ¹H NMR (CDCl₃) δ 7.50–7.32 (m, 12H), 7.28–7.12 (m, 4H), 7.10 (s, 2H), 3.80 (s, 4H), 3.76 (s, 6H); FABMS *m/z* 403 (M⁺ + H), 402 (M⁺).

Dimethyl *N*(4)-Methyl-4,5-dianilinophthalate (2h) and Dimethyl *N*(4), *N*(5)-Dimethyl-4,5-dianilinophthalate (2i). A solution of compound 1 (563 mg, 1.5 mmol), iodomethane (0.93 mL, 15 mmol), and potassium carbonate (442 mg, 3.2 mmol) in dimethylformamide (7 mL) was heated in a sealed tube at 100 °C (48 h). The dark colored solution was taken to dryness. The residue was dissolved in dichloromethane and filtered and the filtrate taken to dryness. The crude mixture of 2h and 2i was separated by several flash chromatographies on silica gel using hexanes and increasing amounts of ethyl acetate as eluent, yielding pure 2h (160 mg, 27.3%) as an amorphous powder [TLC 7.35 (t, 2H, *J* = 7.5 Hz), 7.30–7.05 (m, 5H), 6.87 (t, 1H, *J* = 7.5 Hz), 6.75 (d, 2H, *J* = 7.5 Hz), 6.63 (br s, 1H), 3.89 (s, 3H), 3.81 (s, 3H), 3.25 (s, 3H); FABMS *m/z* 391 (M⁺ + H)] and pure 2i (60

mg, 9.9%) as amorphous powder: TLC (hexanes/ethyl acetate, 3:1) R_f 0.19 (UV); $^1\text{H NMR}$ (CDCl_3) δ 7.55 (s, 2H), 7.14 (t, 4H, $J = 6.0$ Hz), 6.85 (t, 2H, $J = 6.0$ Hz), 6.60 (d, 4H, $J = 6.0$ Hz), 3.88 (s, 6H), 3.05 (s, 6H); FABMS m/z 405 ($\text{M}^+ + \text{H}$).

2-Methyl-1,3-diphenyl-5,6-bis(methoxycarbonyl)benzimidazolium Chloride (2j). A solution of compound 1 (600 mg, 1.59 mmol), acetyl chloride (0.56 mL, 7.95 mmol), and potassium carbonate (0.44 g, 2.98 mmol) in dimethylformamide (10 mL) was heated in a sealed tube at 60 °C (5 h). Insoluble material was filtered off and the filtrate taken to dryness. The crude residue was dissolved in dichloromethane, washed with water, dried over sodium sulfate, and taken to dryness. Crystallization from dichloromethane/ethyl acetate yielded pure 2j (510 mg, 73.5%) as colorless crystals: TLC (dichloromethane/methanol 4:1) R_f 0.23 (UV); $^1\text{H NMR}$ ($\text{DMSO}-d_6$) δ 8.28 (d, 4H, $J = 7.9$ Hz), 7.73 (s, 2H), 7.44 (t, 4H, $J = 7.9$ Hz), 7.36 (t, 2H, $J = 7.9$ Hz), 3.62 (s, 6H), 2.65 (s, 3H); $^{13}\text{C NMR}$ ($\text{DMSO}-d_6$) δ 165.5 s, 156.0 s, 132.4 s, 131.1 d, 130.3 d, 129.8 s, 126.7 d, 113.4 d, 52.6 q, 12.3 q; FABMS m/z 401 (M^+).

Dimethyl 4,5-Bis(*N*-cyclohexylamino)phthalate (2k). A solution of dimethyl 4,5-bis((trimethylsilyloxy)cyclohexa-1,4-dienedicarboxylate (2.24 g, 6 mmol) in cyclohexylamine (21.5 mL, 1.88 mmol) and glacial acetic acid (4.5 mL) was stirred at reflux (3.5 h). The reaction mixture was cooled to room temperature, dissolved in dichloromethane, and extracted with 2 N HCl, saturated NaHCO_3 , and water. The water layers were twice reextracted with dichloromethane. The organic layer were combined, dried with sodium sulfate, filtered, and taken to dryness. The red-brown oil was flash chromatographed on silica gel using hexanes/ethyl acetate (12:5) as eluent. The product fractions were combined and flash chromatographed on silica gel using hexanes/ethyl acetate (4:1) as eluent. The product fractions were combined and taken to dryness. Crystallization from ethyl acetate/hexanes yielded pure 2k as white crystals (657 mg, 28%): mp 158–160 °C; TLC (hexanes/ethyl acetate 4:1) R_f 0.45 (UV); $^1\text{H NMR}$ (CDCl_3) δ 6.90 (s, 2H), 3.85 (s, 6H), 3.38 (br s, 2H), 3.35–3.15 (m, 2H), 2.12–1.95 (m, 4H), 1.85–1.55 (m, 6H), 1.55–1.10 (m, 10H); FABMS m/z 389 ($\text{M}^+ + \text{H}$), 388 (M^+).

4,5-Dianilinophthalamide (3). General Method B. A suspension of dimethyl 4,5-dianilinophthalate (1.08 g, 2.87 mmol) in ethylene glycol (80 mL) was heated to 120 °C, and a steady stream of dry ammonia gas was passed through (16 h). The reaction mixture was cooled to room temperature, diluted with ethyl acetate (160 mL), and mixed with water (160 mL). The aqueous layer was saturated with sodium chloride and separated. The organic layer was extracted with water and brine. The organic phase was dried with sodium sulfate, filtered, and taken to dryness. The residue was absorbed onto silica gel and flash chromatographed on silica gel using hexanes/ethyl acetate (1:1) as eluent. Product fractions were collected and taken to dryness. Crystallization from dichloromethane yielded pure 3 as orange crystals (556 mg, 59%): mp 205–207 °C; TLC (hexanes/ethyl acetate 1:1) R_f 0.29 (UV); $^1\text{H NMR}$ (CDCl_3) δ 7.62 (s, 2H), 7.49 (br s, 1H), 7.35 (dd, 4H, $J_1 = 7.8$ Hz, $J_2 = 8.6$ Hz), 7.10 (d, 2H, $J = 7.8$ Hz), 7.05 (d, 4H, $J = 8.6$ Hz), 5.90 (br s, 2H); $^{13}\text{C NMR}$ ($\text{DMSO}-d_6$) δ 168.8 s, 141.6 s, 138.6 s, 128.9 d, 124.5 s, 121.3 d, 119.0 d, 108.9 d, UV (CH_3CN) λ_{max} 252 nm (sh), 272 nm (ϵ 8400), 300 nm (ϵ 19 200), 398 nm (ϵ 6900); IR (KBr) ν_{max} 3400, 3360, 1760, 1710, 1590, 1510, 1470, 1435, 1355, 1250; FABMS m/z 330 ($\text{M}^+ + \text{H}$). Anal. ($\text{C}_{20}\text{H}_{15}\text{N}_3\text{O}_2$) C, H, N.

4,5-Bis(4-fluoroanilino)phthalimide (4). Compound 4 was prepared from dimethyl 4,5-bis(4-fluoroanilino)phthalate (2) in 53% yield using method B, flash chromatographed on silica gel using hexanes/ethyl acetate (1:1) as eluent, and crystallized from hexanes/ethyl acetate to yield orange crystals: mp 244–246 °C; TLC (hexanes/ethyl acetate, 1:1) R_f 0.38 (UV); $^1\text{H NMR}$ ($\text{DMSO}-d_6$) δ 10.8 (br s, 1H), 7.90 (br s, 2H), 7.29 (s, 2H), 7.25/7.15 (AB, 8H, $J_{\text{AB}} = 7.5$ Hz); $^{13}\text{C NMR}$ ($\text{DMSO}-d_6$) δ 169.6 s, 157.9 s, 139.7 s, 138.6 s, 125.2 s, 122.0 d, 116.3 d, 109.0 d; UV (CH_3CN) λ_{max} 236 nm (ϵ 16 000, sh), 250 nm (ϵ 16 400, sh), 267 nm (ϵ 17 800), 300 nm (ϵ 22 100), 395 nm (ϵ 6500); IR (KBr) ν_{max} 3380, 3310, 1755, 1695, 1595, 1510, 1470, 1350, 1220; FABMS m/z 366 ($\text{M}^+ + \text{H}$). Anal. ($\text{C}_{20}\text{H}_{13}\text{F}_2\text{N}_3\text{O}_2$) C, H, N, F.

4,5-Bis(4-methylanilino)phthalimide (5). Compound 5 was prepared from dimethyl 4,5-bis(4-methylanilino)phthalate (2a) in 41% yield using method B: mp 233–235 °C; TLC (hexanes/

ethyl acetate, 1:1) R_f 0.14 (UV); $^1\text{H NMR}$ ($\text{DMSO}-d_6$) δ 10.68 (br s, 1H), 7.70 (br s, 2H), 7.25 (s, 2H), 7.18/7.08 (AB, 8H, $J = 7.8$ Hz), 3.28 (s, 6H); $^{13}\text{C NMR}$ ($\text{DMSO}-d_6$) δ 168.8 s, 138.7 s, 138.7 s, 130.7 s, 129.3 d, 123.9 s, 119.9 d, 107.6 d, 19.9 q; UV (CH_3CN) λ_{max} 206 nm (sh), 240 nm (ϵ 16 100), 274 nm (ϵ 20 400), 306 nm (ϵ 19 400), 419 nm (ϵ 6200); IR (ν_{max} (CH_2Cl_2) 3700, 3440, 3080–2850, 1770, 1740, 1600, 1530, 1465, 1350; MS m/z 357 (M^+). Anal. ($\text{C}_{22}\text{H}_{19}\text{N}_3\text{O}_2$) C, H, N.

4,5-Bis(4-methoxyanilino)phthalimide (6). Compound 6 was prepared from dimethyl 4,5-bis(4-methoxyanilino)phthalate (2b) in 37% yield using method B, flash chromatographed on silica gel using dichloromethane/ethyl acetate (8:1) as eluent and crystallized from ethyl acetate/hexanes to yield orange crystals: mp 191–193 °C; TLC (hexanes/ethyl acetate, 1:1) R_f 0.44 (UV); $^1\text{H NMR}$ (CDCl_3) δ 7.38 (br s, 1H), 7.36 (s, 2H), 7.03/6.91 (AB, 8H, $J_{\text{AB}} = 9.5$ Hz), 5.69 (br s, 2H), 3.82 (s, 6H); FABMS m/z 390 ($\text{M}^+ + \text{H}$). Anal. ($\text{C}_{22}\text{H}_{19}\text{N}_3\text{O}_4$) C, H, N.

4,5-Bis(4-hydroxyanilino)phthalimide (7). To a solution of compound 6 (1.17 g, 3.0 mmol) in dichloromethane (120 mL) under argon was added a solution of boron tribromide (1.73 mL, 18 mmol) in dichloromethane at room temperature over 40 min. The resulting solution was stirred at room temperature (5 h). The reaction mixture was cooled to 0 °C, and quenched by the careful addition of water (30 mL), and then diluted with ethyl acetate and water. The organic layer was separated and twice extracted with ethyl acetate. The organic phase were combined, washed twice with water and brine, dried over magnesium sulfate, and filtered. A mixture of 0.5 g of ascorbic acid, 0.5 g of sodium ascorbate, and 5 g of silica gel was added and the resulting suspension taken to dryness. The residue was suspended in ethyl acetate/hexanes (5:3), added onto a silica gel column, precoated with 7% (w/w) ascorbic acid, and flash chromatographed using hexanes/ethyl acetate (5:3) as eluent. Product fractions were collected and taken to dryness. Crystallization from ethyl acetate/hexanes yielded pure 7 as dark red crystals (699 mg, 64%): mp 245 °C dec; TLC (hexanes/ethyl acetate, 1:1) R_f 0.30 (UV); HPLC (254 nm) $t_R = 13.25$ min (100%); $^1\text{H NMR}$ ($\text{DMSO}-d_6$) δ 10.60 (br s, 1H), 9.35 (br s, 2H), 7.48 (br s, 2H), 7.05 ($^{1/2}$ AB, 4H, $J = 9.5$ Hz), 6.99 (s, 2H), 6.81 ($^{1/2}$ AB, 4H, $J = 9.5$ Hz); FABMS m/z 362 ($\text{M}^+ + \text{H}$). Anal. ($\text{C}_{20}\text{H}_{15}\text{N}_3\text{O}_4 \cdot 1/4\text{C}_6\text{H}_8\text{O}_2 \cdot 1/2\text{H}_2\text{O}$) C, H, N.

4,5-Bis[4-(*N,N*-diethylamino)anilino]phthalimide (8). Compound 8 was prepared from dimethyl 4,5-bis[4-(*N,N*-diethylamino)anilino]phthalate (2c) in 14% yield using method B, flash chromatographed on silica gel using dichloromethane/methanol (30:1) as eluent, taken to dryness dissolved in dichloromethane, and treated with excess 4 N HCl(g) in diethyl ether to yield yellow crystals: mp 228–230 °C; TLC (dichloromethane/methanol, 30:1) R_f 0.43 (UV); $^1\text{H NMR}$ ($\text{DMSO}-d_6$) δ 8.70 (br s, 2H), 7.65 (AB, 4H, $J_{\text{AB}} = 5.5$ Hz), 7.53 (s, 2H), 7.23 (AB, 4H, $J_{\text{AB}} = 5.5$ Hz), 3.50 (q, 8H, $J_q = 6.5$ Hz), 1.05 (t, 12H, $J_t = 6.5$ Hz); FABMS m/z 472 ($\text{M}^+ + \text{H}$). Anal. ($\text{C}_{28}\text{H}_{33}\text{N}_5\text{O}_2 \cdot 2\text{HCl} \cdot \text{H}_2\text{O}$) C, H, N.

4,5-Bis(4-iodoanilino)phthalimide (9). Compound 9 was prepared from dimethyl 4,5-bis(4-iodoanilino)phthalate (2d) in 32% yield using method B and crystallized from dichloromethane to yield orange needles: mp 246–247 °C (darkening from 235 °C); TLC (dichloromethane) R_f 0.15 (UV); (hexanes/ethyl acetate, 1:1) R_f 0.5 (UV); $^1\text{H NMR}$ (CD_3OD) δ 7.59 (AB, 4H, $J = 10$ Hz), 7.54 (s, 2H), 6.91 (AB, 4H, $J = 10$ Hz); FABMS m/z 582 ($\text{M}^+ + \text{H}$); HRMS ($\text{C}_{20}\text{H}_{13}\text{N}_3\text{O}_2\text{I}_2$).

4,5-Bis(4-cyanoanilino)phthalimide (10). A yellow suspension of compound 9 (208 mg, 0.36 mmol) and copper(I) cyanide in dimethylformamide under dry argon was stirred at 140 °C (5 h) and then cooled to 70 °C, and ethyl acetate (3 mL) was added. A solution of iron (III) chloride (168 mg, 1.04 mmol) in water (0.6 mL) and concentrated HCl (0.6 μL) was added at 65–70 °C to the reaction mixture. The mixture was stirred at reflux (30 min), cooled to 40 °C, treated with Hyflo, and filtered. The filtrate was separated into two phases, and the organic phase was extracted with water, brine, and again with water. The water layers were reextracted once with ethyl acetate. The organic layers were combined, dried over magnesium sulfate, filtered, and taken to dryness. The residue was flash chromatographed on silica gel using hexanes/ethyl acetate (2:3) as eluent. Product fractions were collected and taken to dryness. Crystallization from ethyl acetate/dichloromethane yielded pure 10 as slightly

green crystals (15 mg, 11%): mp >240 °C; TLC (ethyl acetate/hexanes, 1:1) R_f 0.44 (UV); $^1\text{H NMR}$ (DMSO- d_6) δ 8.87 (br s, 2H), 7.68 (s, 2H), 7.62 (AB, 4H, $J = 9$ Hz), 7.13 (AB, 4H, $J = 9$ Hz); FABMS m/z 380 ($\text{M}^+ + \text{H}$); HRMS ($\text{C}_{22}\text{H}_{13}\text{N}_5\text{O}_2$).

4,5-Bis(4-phenylanilino)phthalimide (11). Compound 11 was prepared from dimethyl 4,5-bis(4-phenylanilino)phthalate (2e) in 17% yield using method B, flash chromatographed on silica gel using dichloromethane/ethyl acetate (2:1) as eluent, and crystallized from dichloromethane/hexanes: mp 230–231 °C; TLC (dichloromethane/ethyl acetate, 2:1) R_f 0.55 (UV); $^1\text{H NMR}$ (CDCl_3) δ 7.68 (s, 2H), 7.59 (d, 8H, $J = 5.0$ Hz), 7.45 (t, 4H, $J = 5.0$ Hz), 7.40–7.30 (m, 4H), 7.14 (d, 4H, $J = 5.0$ Hz), 5.96 (br s, 2H); FABMS m/z 482 ($\text{M}^+ + \text{H}$). Anal. ($\text{C}_{32}\text{H}_{23}\text{N}_3\text{O}_2 \cdot 1.2\text{H}_2\text{O}$) C, H, N.

4-(Methoxyanilino)-5-anilinophthalimide (12). Compound 12 was prepared from dimethyl 4-(methoxyanilino)-5-anilinophthalate (2f) in 48% yield using method B, flash chromatographed on silica gel using hexanes/ethyl acetate (3:2) as eluent, and crystallized from ethyl acetate/diethyl ether to yield yellow crystals: mp 183–185 °C; TLC (ethyl acetate/hexanes 1:1) R_f 0.52 (UV); $^1\text{H NMR}$ (DMSO- d_6) δ 10.72 (br s, 1H), 7.82 (br s, 1H), 7.75 (br s, 1H), 7.38 (s, 1H), 7.35 (t, 2H, $J = 7.2$ Hz), 7.20 (d, 2H, $J = 7.2$ Hz), 7.16 (s, 1H), 7.14/7.00 (AB, 4H, $J = 10$ Hz), 6.98 (t, 1H, $J = 7.2$ Hz); FABMS m/z 360 ($\text{M}^+ + \text{H}$). Anal. ($\text{C}_{21}\text{H}_{17}\text{N}_3\text{O}_3$) C, H, N.

5,8-Diphenyl-5,8-diaza-5,6,7,8-tetrahydronaphthalene-2,3-dicarboximide (13). Compound 13 was prepared from dimethyl 5,8-diphenyl-5,8-diaza-5,6,7,8-tetrahydronaphthalene-2,3-dicarboxylate (2g) in 33% yield using method B yielding yellow amorphous powder after flash chromatography: TLC (dichloromethane/methanol, 20:1) R_f 0.55 (UV); $^1\text{H NMR}$ (CDCl_3) δ 7.45 (t, 2H, $J = 6.0$ Hz), 7.43 (d, 4H, $J = 6.0$ Hz), 7.29 (d, 4H, $J = 6.0$ Hz), 7.10 (br s, 1H), 7.04 (s, 2H), 3.86 (s, 4H); FABMS m/z 356 ($\text{M}^+ + \text{H}$); HRMS ($\text{C}_{22}\text{H}_{17}\text{N}_3\text{O}_2$).

N(4)-Methyl-4,5-dianilinophthalimide (14). Compound 14 was prepared from dimethyl *N*(4)-methyl-4,5-dianilinophthalate (2h) in 15.6% yield using method B to yield a yellow powder: mp 150–155 °C; TLC (hexanes/ethyl acetate 3:1) R_f 0.17 (UV); $^1\text{H NMR}$ (CDCl_3) δ 7.63 (s, 1H), 7.58 (s, 1H), 7.45–7.05 (m, 6H), 7.00–6.70 (m, 4H), 3.27 (s, 3H); FABMS m/z 344 ($\text{M}^+ + \text{H}$); HRMS ($\text{C}_{21}\text{H}_{17}\text{N}_3\text{O}_2$).

N(4),N(5)-Dimethyl-4,5-dianilinophthalimide (15). Compound 15 was prepared from dimethyl *N*(4)-methyl-4,5-dianilinophthalate (2i) in 22.6% yield using method B: TLC (hexanes/ethyl acetate, 3:1) R_f 0.14 (UV); $^1\text{H NMR}$ (CDCl_3) δ 7.64 (s, 2H), 7.16 (t, 4H, $J = 7.0$ Hz), 6.87 (t, 2H, $J = 7.0$ Hz), 6.60 (d, 4H, $J = 7.0$ Hz), 3.08 (s, 6H); FABMS m/z 358 ($\text{M}^+ + \text{H}$).

N(4)-Acetyl-4,5-dianilinophthalimide (16). Compound 16 was prepared from 2-methyl-1,3-diphenyl-5,6-bis(methoxycarbonyl)benzimidazolium chloride (2j) in 8.9% yield using method B: mp >240 °C (darkening from 160 °C); TLC (hexanes/ethyl acetate, 1:1) R_f 0.33 (UV); $^1\text{H NMR}$ (DMSO- d_6) δ 8.15 (br s, 1H), 7.69 (s, 1H), 7.60 (br s, 1H), 7.55 (d, 2H, $J = 7.2$ Hz), 7.38 (t, 2H, $J = 6.6$ Hz), 7.33 (t, 2H, $J = 6.6$ Hz), 7.28–7.08 (m, 5H), 2.06 (s, 3H); FABMS m/z 372 ($\text{M}^+ + \text{H}$); HRMS ($\text{C}_{22}\text{H}_{17}\text{N}_3\text{O}_3$).

4,5-Dianilinophthalanilide (17). Compound 17 was isolated as byproduct from the mother liquor of compound 1 by flash chromatography and was crystallized from ethyl acetate/hexanes to yield yellow crystals in <1% yield: mp 184–185 °C; TLC (hexanes/ethyl acetate 2:1) R_f 0.5 (UV); $^1\text{H NMR}$ (CDCl_3) δ 7.72 (s, 2H), 7.53–7.33 (m, 9H), 7.15–7.05 (m, 6H), 5.93 (br s, 2H); $^{13}\text{C NMR}$ (CDCl_3) δ 167.7 s, 141.7 s, 140.4 s, 132.6 s, 130.2 d, 129.3 d, 128.0 d, 126.9 d, 126.0 s, 123.6 d, 120.1 d, 112.9 d; UV (CH_3CN) λ_{max} 248 (ϵ 20 000), 288 (sh), 317 (ϵ 25 200), 424 nm (ϵ 5800); IR (CH_2Cl_2) ν_{max} 3380, 3040, 1780, 1720, 1590, 1500, 1470, 1450, 1430, 1375, 1325, 1260; MS m/z 405 (M^+). Anal. ($\text{C}_{26}\text{H}_{19}\text{N}_3\text{O}_2$) C, H, N.

N-Methyl-4,5-dianilinophthalimide (18). Compound 18 was isolated as byproduct from the flash chromatography of compound 3 and was crystallized from dichloromethane to yield yellow crystals in <0.1% yield: mp 195–196 °C; TLC (hexanes/ethyl acetate, 1:2) R_f 0.77 (UV); $^1\text{H NMR}$ (DMSO- d_6) δ 7.97 (br s, 2H), 7.43 (s, 2H), 7.35 (t, 4H, $J = 7.5$ Hz) 7.18 (d, 4H, $J = 7.5$ Hz), 7.02 (t, 2H, $J = 7.5$ Hz), 2.96 (s, 3H); FABMS m/z 344 ($\text{M}^+ + \text{H}$). Anal. ($\text{C}_{21}\text{H}_{17}\text{N}_3\text{O}_2$) C, H, N.

4,5-Bis(*N*-cyclohexylamino)phthalimide (19). Compound 19 was prepared from dimethyl 4,5-bis(*N*-cyclohexylamino)phthalate (2k) in 28% yield using method B, flash chromatographed on silica gel using hexanes/ethyl acetate (2:1) as eluent, and crystallized from dichloromethane to yield yellow crystals: mp 198–201 °C; TLC (hexanes/ethyl acetate, 2:1) R_f 0.5 (UV); $^1\text{H NMR}$ (CDCl_3) δ 7.15 (br s, 1H), 7.00 (s, 2H), 3.50 (br m, 2H), 3.41–3.23 (br m, 2H), 2.15–2.00 (m, 4H), 1.90–1.65 (m, 6H), 1.55–1.10 (m, 10H); FABMS m/z 342 ($\text{M}^+ + \text{H}$). Anal. ($\text{C}_{20}\text{H}_{27}\text{N}_3\text{O}_2$) C, H, N.

4,5-Bis(phenylthio)-1,2,3,6-tetrahydrophthalimide (20). A solution of 3,4-bis(phenylthio)sulfolene (335 mg, 1 mmol) and maleimide (117 mg, 1.2 mmol) in *p*-xylene (10 mL) was stirred at reflux (12 h). The reaction mixture was cooled to room temperature and taken to dryness. The dark brown residue was dissolved in ethyl acetate and extracted with water and brine. The organic phase was dried with sodium sulfate, filtered, and concentrated to 20 mL. Crystallization in the freezer yielded pure 20 as white crystals (222 mg, 60.4%): TLC (ethyl acetate/hexanes, 2:1) R_f 0.55 (UV); $^1\text{H NMR}$ (CDCl_3) δ 7.85 (br s, 1H), 7.42–7.30 (m, 10H), 3.12 (m, 2H), 2.76–2.40 (m, 4H); FABMS m/z 368 ($\text{M}^+ + \text{H}$).

4,5-Bis(phenylthio)phthalimide (21). A solution of 4,5-bis(phenylthio)-1,2,3,6-tetrahydrophthalimide (20) (146 mg, 0.4 mmol) and DDQ (200 mg, 0.88 mmol) in toluene (10 mL) was stirred at reflux (7 h). The reaction mixture was cooled to room temperature and filtered, and the filtrate was taken to dryness. The brown residue was flash chromatographed on silica gel using hexanes/ethyl acetate (2:1) as eluent. Product fractions were collected and taken to dryness to yield pure amorphous 21 as brown powder (15 mg, 10%): mp 200–202 °C; TLC (hexanes/ethyl acetate, 2:1) R_f 0.66 (UV); $^1\text{H NMR}$ (CDCl_3) δ 7.62–7.43 (m, 10H), 7.38 (br s, 2H), 7.29 (s, 2H); FABMS m/z 364 ($\text{M}^+ + \text{H}$); HRMS ($\text{C}_{20}\text{H}_{14}\text{NO}_2\text{S}_2$).

Crystal Structure Analysis of Compound 3. An orange-colored needle-shaped crystal of $\text{C}_{20}\text{H}_{15}\text{N}_3\text{O}_2 \cdot 0.5 \text{CH}_3\text{OH}$ having approximate dimensions of $0.65 \times 0.18 \times 0.08$ mm was mounted on a glass fiber. All measurements were made on an Enraf-Nonius CAD4 diffractometer with graphite monochromated $\text{Cu K}\alpha$ radiation. The crystal belongs to the monoclinic space group $P2_1/n$ with $a = 10.937(1)$ Å, $b = 10.017(2)$ Å, $c = 15.966(2)$ Å, $\beta = 100.78(1)^\circ$, $V = 1718(1)$ Å 3 , $Z = 4$, $D_{\text{calc}} = 1.335$ g/cm 3 . The intensities were corrected for Lorentz and polarization effects but not for absorption ($\mu = 6.465$ cm $^{-1}$). A total of 3884 independent intensities were measured of which 2030 were classified as observed with $I > 3\sigma(I)$. The structure was solved by direct methods using the computer program MULTAN80.⁵⁴ All hydrogen atom positions were located from difference Fourier maps except those of the disordered solvent molecule. The structure was refined using full-matrix least-squares calculations with anisotropic displacement parameters for non-hydrogen atoms and fixed ones for hydrogen atoms. The final R factor for 302 variables was 0.075, and the goodness of fit was 1.97. The highest peak in the final difference Fourier map was 0.63 e/Å 3 . Positional and thermal parameters, bond lengths, and bond angles have been deposited as supplementary material.

Acknowledgment. We gratefully acknowledge the excellent technical assistance of B. Adam, J. Bohn, U. Dürler, C. Kölbing, N. Martin, V. Rigo, J. Schittly, K. Stoll, H. Walter, and F. Wenger. We thank Dr. H. Fuhrer, O. Hosang, and F. Raschdorf for spectral measurements and Dr. E. McGlynn, J. Liebetanz, B. Gay, M. Becker, and S. Reutener for expression and purification of the EGF-R ICD and *c-src* kinases.

Supplementary Material Available: Positional and thermal parameters, bond lengths and bond angles of the crystal structure of compound 3 (6 pages). Ordering information is given on any current masthead page.

References

- (1) Carpenter, G. Receptors for Epidermal Growth Factor and other Polypeptide Mitogens. *Annu. Rev. Biochem.* 1987, 56, 881–914.

- (2) Yarden, Y.; Ullrich, A. Growth Factor Receptor Tyrosine Kinases. *Annu. Rev. Biochem.* 1988, 57, 443-478.
- (3) Ullrich, A.; Schlessinger, J. Signal Transduction by Receptors with Tyrosine Kinase Activity. *Cell* 1990, 61, 203-212.
- (4) Chen, W. S.; Lazar, C. S.; Poenie, M.; Tsien, R. J.; Gill, G. N.; Rosenfeld, M. G. Requirement for Intrinsic Protein Tyrosine Kinase in the Immediate and Late Actions of the EGF-Receptor. *Nature (London)* 1987, 328, 820-823.
- (5) Honegger, A. M.; Dull, T. J.; Felder, S.; Van Obberghen, E.; Bellot, F.; Szapary, D.; Schmidt, A.; Ullrich, A.; Schlessinger, J. Point Mutation at the ATP Binding Site of the EGF Receptor Abolishes Protein-Tyrosine Kinases Activity and Alters Cellular Routing. *Cell* 1987, 51, 199-209.
- (6) Gullick, W. J. Prevalence of Aberrant Expression of the Epidermal Growth Factor Receptor in Human Cancers. *Br. Med. Bull.* 1991, 47, 87-98.
- (7) Aaronson, S. A. Growth Factors and Cancer. *Science* 1991, 254, 1146-1152.
- (8) Hynes, N. E. Amplification and Overexpression of the c-erbB-2 Gene in Human Tumors: its Involvement in Tumor Development, its Significance as a Prognostic Factor, and its Potential as a Target for Cancer Therapy. *Seminars Cancer Biol.* 1993, 4, 19-26.
- (9) Velu, T. J.; Beguinot, L.; Vass, W. C.; Willingham, M. C.; Merlino, G. T.; Pastan, I.; Lowy, D. R. Epidermal Growth Factor-dependent Transformation by a Human EGF Receptor Proto-Oncogene. *Science* 1987, 238, 1408-1410.
- (10) Di Fiore, P. P.; Pierce, J. H.; Flemming, T. P.; Hazan, R.; Ullrich, A.; King, C. R.; Schlessinger, J.; Aaronson, S. A. Overexpression of the Human EGF Receptor Confers an EGF-Dependent Transformed Phenotype to NIH 3T3 Cells. *Cell* 1987, 51, 1063-1070.
- (11) Di Fiore, P. P.; Pierce, J. H.; Kraus, M. H.; Segatto, O.; King, C. R.; Aaronson, S. A. ErgB-2 is a Potent Oncogene when Overexpressed in NIH 3T3 Cells. *Science* 1987, 237, 178-182.
- (12) Vasser, R.; Hutton, M. E.; Fuchs, E. Transgenic Overexpression of Transforming Growth Factor Alpha Bypasses the Need for c-Ha-ras Mutations in Mouse Skin Tumorigenesis. *Mol. Cell. Biol.* 1992, 12, 4643-4653.
- (13) Sandgren, E.; Luetteke, N. C.; Palmiter, R. D.; Brinster, R. L.; Lee, D. C. Overexpression of TGF Alpha in Transgenic Mice: Induction of Epithelial Hyperplasia, Pancreatic Metaplasia, and Carcinoma of the Breast. *Cell* 1990, 61, 1121-1135.
- (14) Schreiber, A. B.; Winkler, M. E.; Derynck, R. Transforming Growth Factor Alpha: a more Potent Angiogenic Mediator than Epidermal Growth Factor. *Science* 1986, 232, 1250-1253.
- (15) Burke, T. R. Protein-Tyrosine Kinase Inhibitors. *Drugs Future* 1992, 17, 119-131.
- (16) Reugg, U. T.; Burgess, G. M. Staurosporine, K-252 and UNC-01: Potent but Nonspecific Inhibitors of Protein Kinases. *Trends Pharmacol. Sci.* 1989, 10, 218-220.
- (17) Tamaoki, T.; Nomoto, H.; Takahashi, I.; Kato, Y.; Morimoto, M.; Tomita, F. Staurosporine, a Potent Inhibitor of Phospholipid/Ca⁺⁺ Dependent Protein Kinase. *Biochem. Biophys. Res. Commun.* 1986, 135, 397.
- (18) Meyer, T.; Regenass, U.; Fabbro, D.; Alteri, E.; Roesel, J.; Muller, M.; Caravatti, G.; Matter, A. A Derivative of Staurosporine (CGP 41 251) Shows Selectivity for Protein Kinase C Inhibition and In Vitro Proliferative as well as In Vivo Anti-Tumor Activity. *Int. J. Cancer* 1989, 43, 851-856.
- (19) Ward, N. E.; O'Brian, C. A. Kinetic Analysis of Protein Kinase C Inhibition by Staurosporine: Evidence that Inhibition Entails Inhibitor Binding at a Conserved Region of the Catalytic Domain but not Competitive with Substrate. *Mol. Pharmacol.* 1991, 41, 387-392.
- (20) Davis, P. D.; Hill, C. H.; Keech, E.; Lawton, G.; Nixon, J. S.; Sedgwick, A. D.; Wadsworth, J.; Westmacott, D.; Wilkinson, S. E. The Design of Inhibitors of Protein Kinase C: The Solution Conformation of Staurosporine. *FEBS Lett.* 1989, 259, 61.
- (21) Toullec, D.; Pianetti, P.; Coste, H.; Bellevergue, P.; Grand-Perret, T.; Ajakane, M.; Baudet, V.; Boissin, P.; Boursier, E.; Loriolle, F.; Duhamel, L.; Charon, D.; Kirilovsky, J. The Bisindolylmaleimide GF 109203X is a Potent and Selective Inhibitor of Protein Kinase C. *J. Biol. Chem.* 1991, 266, 15771-15781.
- (22) Bit, R. A.; Davis, P. D.; Elliott, L. H.; Harris, W.; Hill, C. H.; Keech, E.; Kumar, H.; Lawton, G.; Maw, A.; Nixon, J. S.; Vesey, D. R.; Wadsworth, J.; Wilkinson, S. E. Inhibitors of protein kinase C. 3. Potent and Highly Selective Bisindolylmaleimides by Conformational Restriction. *J. Med. Chem.* 1993, 36, 21-29.
- (23) Matlin, S. A.; Barron, K. Reactions of 1,2-Bis(trimethylsilyloxy)cyclohexenes with Amines. *J. Chem. Res. Synop.* 1990, 8, 246-247.
- (24) Mowry, D. T. The Preparation of Nitriles. *Chem. Rev.* 1948, 42, 189-283.
- (25) Chou, T.-S.; Lee, S.-J.; Peng, M.-L.; Sun, D.-J.; Chou, S.-S. Preparation of 2,3-Dihetero-Substituted 1,3-Dienes from Brominated 2-Sulfolenes. *J. Org. Chem.* 1988, 53, 3027-3031.
- (26) Hopkins, P. B.; Fuchs, P. L. Chlorosulfonylation-Dehydrochlorination Reactions. New Improved Methodology for the Synthesis of Unsaturated Aryl Sulphides and Aryl Sulfoxes. *J. Org. Chem.* 1978, 43, 1206-1217.
- (27) McGlynn, E.; Becker, M.; Mett, H.; Reutener, S.; Cozens, R.; Lydon, N. B. Large Scale Purification and Characterization of a Recombinant Epidermal Growth Factor Receptor Protein Tyrosine Kinase. *Eur. J. Biochem.* 1992, 207, 265-275.
- (28) Richert, N. D.; Blithe, D. L.; Pastan, I. Properties of the src Kinase Purified from Rous Sarcoma Virus-Infected Rat Tumors. *J. Biol. Chem.* 1982, 257, 714350-7150.
- (29) Faulkes, J. G.; Chow, M.; Gorka, C.; Frackelton, A. R.; Baltimore, D. Purification and Characterization of a Protein-Tyrosine Kinase Encoded by the Abelson Murine Leukemia Virus. *J. Biol. Chem.* 1985, 260, 8070-8077.
- (30) Graziani, Y.; Erikson, R. L. Characterization of the Rous Sarcoma Virus Transforming Gene Product. *J. Biol. Chem.* 1983, 258, 6344-6351.
- (31) Pritchard, M. L.; Rleman, D.; Field, J.; Kruse, C.; Rosenberg, M.; Poste, G.; Greig, R. G.; Ferguson, B. Q. A Truncated v-abl Tyrosine-Specific Tyrosine Kinase Expressed in E. coli. *Biochem. J.* 1989, 257, 321-329.
- (32) Shu, H.-K. G.; Pelly, R. J.; Kung, H.-J. Tissue-Specific Transformation by Epidermal Growth Factor Receptor: A Single Point Mutation within the ATP-binding Pocket of the erbB Product Increases its Intrinsic Protein Kinase Activity and Activates its Sarcomagenic Potential. *Proc. Natl. Acad. Sci. U.S.A.* 1990, 87, 9103-9107.
- (33) Hanks, S. K.; Quinn, A. M.; Hunter, T. The Protein Kinase Family: Conserved Features and Phylogeny of the Catalytic Domains. *Science* 1988, 241, 42-52.
- (34) Furusaki, A.; Hashiba, N.; Matsumoto, T.; Hirano, A.; Iwai, Y.; Omura, S. The Crystal and Molecular Structure of Staurosporine, a New Alkaloid from a Streptomyces Strain. *Bull. Chem. Soc. Jpn.* 1982, 55, 3681-3685.
- (35) Downward, J.; Parker, P.; Waterfield, M. D. Autophosphorylation Sites on the Epidermal Growth Factor Receptor. *Nature (London)* 1984, 311, 483-485.
- (36) Weber, W.; Bertics, P. J.; Gill, G. N. Immunoaffinity Purification of the Epidermal Growth Factor Receptor. *J. Biol. Chem.* 1984, 259, 14631-14636.
- (37) Donaldson, R. W.; Cohen, S. Epidermal Growth Factor Stimulates Tyrosine Phosphorylation in the Neonatal Mouse: Association of a Mr 55,000 Substrate with the Receptor. *Proc. Natl. Acad. Sci. U.S.A.* 1992, 89, 8477-8481.
- (38) Bertics, P. J.; Gill, G. N. Self-Phosphorylation Enhances the Tyrosine Protein Kinase Activity of the EGF-Receptor. *J. Biol. Chem.* 1985, 260, 14642-14647.
- (39) Bertics, P. J.; Chen, W. S.; Hubler, L.; Lazar, C. S.; Rosenfeld, M. G.; Gill, G. N. Alteration of EGF-Receptor Activity by Mutation of its Primary Carboxyl-Terminal Site of Tyrosine Self-Phosphorylation. *J. Biol. Chem.* 1988, 263, 3610-3617.
- (40) Schlessinger, J.; Ullrich, A. Growth Factor Signaling by Receptor Tyrosine Kinases. *Neuron* 1992, 9, 383-391.
- (41) Greenburg, M. E.; Ziff, E. B. Stimulation of 3T3 Cells Induces Transcription of the c-fos Proto-Oncogene. *Nature (London)* 1984, 311, 433-437.
- (42) Kruijer, W.; Cooper, J. A.; Hunter, T.; Verma, I. M. Platelet-Derived Growth Factor Induces Rapid but Transient Expression of the c-fos Gene and Protein. *Nature (London)* 1984, 312, 711-716.
- (43) Giard, D. J.; Aaronson, S. A.; Todaro, G. J.; Arnstein, P.; Kersey, J. H.; Dosik, H.; Parks, W. P. In Vitro Cultivation of Human Tumors: Establishment of Cell Lines Derived From a Series of Solid Tumors. *J. Natl. Cancer Inst.* 1973, 51, 1417-1423.
- (44) King, C. R.; Kraus, M. H.; Williams, L. T.; Merlino, G. T.; Pastan, I.; Aaronson, S. A. Human Cell Lines with EGF Receptor Gene Amplification in the Absence of Aberrant Sized mRNAs. *Nucl. Acids Res.* 1985, 13, 8447-8486.
- (45) Smith, G. E.; Summers, M. D.; Frazer, M. J. Production of Human Beta Interferon in Insect Cells Infected with a Baculovirus Expression Vector. *Mol. Cell. Biol.* 1983, 3, 2156-2165.
- (46) Weissman, B. E.; Aaronson, S. A. BALB and Kirsten Murine Sarcoma Viruses Alter the Growth and Differentiation of EGF-dependent BALB/c Mouse Epidermal Keratinocyte Lines. *Cell.* 1983, 32, 599-606.
- (47) Buchdunger, E.; Trinks, U.; Mett, H.; Regenass, U.; Muller, M.; Meyer, T.; McGlynn, E.; Pinna, L. A.; Traxler, P.; Lydon, N. B. 4,5-Dianilino-phthalimides: a Novel Group of Tyrosine Protein Kinase Inhibitors with Selectivity for the EGF-Receptor Signal Transduction Pathway and Potent In Vivo Antitumor Activity. *Proc. Natl. Acad. Sci. U.S.A.* 1994, in press.
- (48) Lydon, N. B.; Gay, B.; Mett, H.; Murray, B.; Liebetanz, J.; Gutzwiller, A.; Piwnicka-Worms, H.; Roberts, T. M.; McGlynn, E. Purification and Biochemical Characterization of Non-Myristoylated Recombinant pp60 c-SRC. *Biochem. J.* 1992, 287, 985-993.

- (49) Lydon, N. B.; Adams, B.; Poschet, J. F.; Gutzwiller, A.; Matter, A. An *E. coli* Expression system for the Rapid Purification and Characterization of a v-abl Tyrosine Protein Kinase. *Oncogene Res.* 1990, 5, 161-173.
- (50) Geissler, J. F.; Traxler, P.; Regenass, U.; Murray, B.; Roesel, J.; Meyer, T.; McGlynn, E.; Storni, A.; Lydon, N. B. Thiazolidinediones: Biochemical and Biological Activity of a Novel Class of Tyrosine Protein Kinase Inhibitors. *J. Biol. Chem.* 1990, 265, 22255-22261.
- (51) Bradford, M. M. A Rapid and Sensitive Method for the Quantitation of Microgram Quantities of Protein Utilizing the Principle of Protein-Dye Binding. *Anal. Biochem.* 1976, 72, 248-254.
- (52) Druker, T. M.; Mamon, H. J.; Roberts, T. M. Oncogenes, Growth factors, and Signal Transduction. *N. Engl. J. Med.* 1989, 321, 1383-1391.
- (53) Evans, B. D.; Smith, I. E.; Shorthouse, A. J.; Millar, J. J. A Comparison of the Response of Human Lung Cell Carcinoma to Vindesine and Vincristine. *Br. J. Cancer* 1982, 45, 466-468.
- (54) Main, P.; Fiske, S. J.; Hull, S. E.; Lessinger, L.; Germain, G.; Declercq, J. P.; Woolfson, M. M. *MULTAN80. A System of Computer Programs for the Automatic Solution of Crystal Structures from X-ray Diffraction Data*; University of York, England and Louvain, Belgium, 1980.
- (55) Chomczynski, P.; Sacchi, N. Single Step Method of RNA Isolation by Acid Guanidium Thiocyanate-Phenol-Chloroform Extraction. *Anal. Biochem.* 1987, 162, 146-159.
- (56) Curran, T.; Peters, G.; Van Beveren, C.; Teich, N. M.; Verma, I. M. FBJ Murine Osteosarcoma Virus: Identification and Molecular Cloning of Biologically Active Proviral DNA. *J. Virol.* 1982, 44, 674-682.